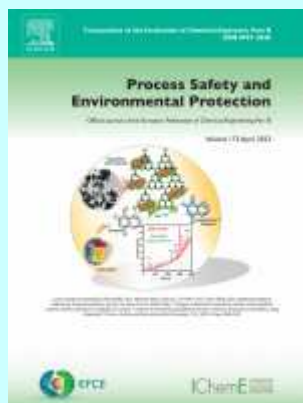


Process Safety and Environmental Protection

Rok 2023, Volume 175

July



Yang Wang, Hong Hao, Wensu Chen, Jingde Li, Zitong Wang. *Prediction of BLEVE loading on a rigid structure.* Pages 1-16.

Boiling Liquid Expanding Vapour Explosion (BLEVE) in open space has been investigated in the authors' previous study. However, for designing structures against BLEVE event, BLEVE load acting on structures, instead of the pressure in open space, should be used in the structural response analysis. Therefore, further study is required to accurately predict BLEVE loads on structures. In this study, 1300 sets of BLEVE cases consisting of 650 wave propagation in open space and 650 pressure wave-structure interaction cases are numerically modelled. The open space BLEVE pressure and reflected pressure waves from the rigid structure are simulated, and the corresponding impulses are calculated. The reflection coefficient chart is developed to predict the reflected BLEVE overpressure on the rigid structure. The diffraction and clearing effects on the reflected waves are analysed with respect to the dimensions of the structure. An empirical formula for predicting the reflected impulse is also proposed. The results obtained in this study can be used together with the open space BLEVE pressure predictions presented by the authors in a previous study to predict the BLEVE loads on structures.

- **Keywords:** BLEVE; Reflected overpressure; Reflection coefficient; Diffraction; Clearing time; Reflected impulse

Mengxuan Zhang, Zhe Yang, Yunpeng Zhao, Mingzhu Lv, Xingying Lan, Xiaogang Shi, Jinsen Gao, Chuankun Li, Zhuang Yuan, Yang Lin. *A hybrid safety monitoring framework for industrial FCC disengager coking rate based on FPM, CFD, and ML.* Pages 17-33.

This work proposed a hybrid modeling framework for the safety monitoring of coking rates in FCC (Fluidized Catalytic Cracking) disengager. The framework combines CFD (Computational Fluid Dynamics), coking FPM (First Principles Model), machine learning, and industrial data to establish a comprehensive and customizable approach. The FPM of the coking rate, including the UNIFAC condensation ratio model, the coking ratio model and the capture ratio model, are established by combustion experiments, gas-solid two-phase flow simulations and DPM (Discrete Phase Model) simulations. The capture ratio

model is built to calculate the capture ratio of heavy oil droplets by each high-risk region, achieved by DPM simulation. By establishing a link between the simulated position and the DCS (Distributed Control System) sensor, the simulation results and the real-time DCS data are matching. An improved LSTM (Long Short-Term Memory) network was then established to predict the real-time temperature and pressure in the high-risk coking regions of the disengager using real-time DCS and LIMS (Laboratory Information Management System) data. The LSTM network can achieve online monitoring of coking rate by coupling FPM. This hybrid coking monitoring framework has been industrially applied and validated with an accuracy of over 90% in a continuous one-month online monitoring task, which is highly interpretable and extensible, providing refining companies with a scalable and customizable approach to monitor coking problems in FCC disengager.

- **Keywords:** FCC disengager; Safety monitoring; Coking problem; Industrial applications; Hybrid modeling; CFD simulation

Xingyan Cao, Zhi Wang, Zhirong Wang, Yawei Lu, Shaochen Sun, Jianjun Xu. *Experimental research on the flame resistance characteristics of wire mesh for syngas explosion. Pages 34-47.*

The flame resistance characteristics of wire mesh and its influence factor on syngas explosion were researched by experiment. Relationships between flame propagation and pressure rise at the flame resistance system two ends were clarified under different flame resistance results. And the effect of syngas concentration on explosion parameters was obtained and flame resistance mechanism was also revealed. Results indicate that the existence of wire mesh could indirectly affect pressure rise by affecting the flame propagation, and flame propagation and pressure rise presented a clear corresponding relationship. The wire mesh could play a better inhibiting role and reduce the explosion intensity, affecting by syngas concentration. As the flame resistance failed ($c=30\%$), ΔP_{max} was effectively decreased from 0.81 MPa to 0.52 MPa above wire mesh and from 0.58 MPa to 0.39 MPa below wire mesh. And the reduction extent was more significant under flame resistance success (80.25% and 68.97%). With reduction of syngas concentration and increase of mesh layer, explosion parameters were evidently decreased. Especially the temperature above wire mesh did not present an increase trend and reach the ignition point of syngas under flame resistance success. The inhibition mechanism was mainly attributed to the combination of endothermic and wall effects.

- **Keywords:** Syngas explosion; Wire mesh; Flame resistance characteristics; Flame temperature; Corresponding relationship

Shenglin Bu, Wenzong Liu, Muhammad Rizwan Haider, Xiqi Li, Wenzhe Zhang, Qi Sun, Qiandi Wang, Yuanqiang Guo, Shichen Nie, Aijie Wang. *Expandable polystyrene waste modified iron sludge-based biochar activating multiple free radicals for deep wastewater treatment. Pages 48-59.*

Fe-containing sludge can be converted to functional biochar as a promising resource recycle pathway. However, activating properties of Fe sludge-based biochar are always limited by low specific surface area and weak carbon center for persistent free radical(PFRs). In the current study, waste expandable polystyrene particles were simultaneously used to improve the biochar catalytic performance. The co-prepared biochar achieved a high micromesoporous ratio(98.4%) with specific surface area (345.3 m²/g), improved by 20.1% and 105.2% than unimproved biochar. The improved micromesoporous properties performed better iron active sites and oxygen-containing functional groups for PFRs functioning in wastewater. The co-prepared biochar showed an efficient catalytic degradation through persulfate activating multiple free radicals of 10²,

O_2^{2-} , OH^- and SO_4^{2-} , which removed 95.4% sulfamethoxazole with mineralizing ratio of 74% within 60 min. The recycling of waste iron sludge and waste polystyrene foam material can achieve functional biochar to apply in deep treatment of refractory organic wastewater.

- **Keywords:** Iron sludge; Waste expandable polystyrene; Biochar; Sulfamethoxazole; Catalytic degradation

Mingfei Xing, Xiaofang Wu, Zixin Li, Fan Zhang, Yaping Wang, Li Zhao. *Rare earth element recovery and aluminum-rich residue production from high alumina fly ash by alkali pre-desilication enhance the mechanochemical extraction process. Pages 60-69.*

Recycling rare earth elements (REEs) from coal fly ash by conventional acid leaching may generate large amounts of harmful waste acid, and the obtained acid residues have low utilization value. Accordingly, a green non-acid leaching approach for REE recovery and Al-rich residue production from high alumina fly ash (HAFA) was developed based on the alkali pre-desilication enhanced mechanochemical extraction process. REEs mainly existed in the chemically stable amorphous aluminosilicate glass phase of HAFA, which hindered the leaching of REEs. Thus, NaOH solution (150 g/L) was used to dissolve the glass phase and release REEs from the glass phase under a mild condition (80 °C, 2 h). The released REEs could be easily extracted by green EDTA during the mechanochemical extraction process. The extraction rates of La, Ce, Pr and Nd were about 82.03–88.71%, and valuable Al-rich residue (68.23% Al_2O_3 content and 2.51 Al/Si ratio) can be obtained when the mass ratio of the pre-desilication residue to EDTA, milling time, rotary speed, and liquid-solid ratio were 2:3, 2 h, 500 rpm, and 0.8, respectively. The used EDTA and REEs in the extracted solutions can be recycled by pH adjusting and organic solvent extraction. Thus, this study provides a new idea for green and high-value utilization of HAFA.

- **Keywords:** High alumina fly ash; Rare earth recovery; Alkali pre-desilication; Mechanochemical extraction; EDTA

Yunsung Yoo, Dongwoo Kang. *Inorganic CO₂ conversion through reaction with concentrated reject brine: Polymorphic characteristics of intermediate carbonate salts. Pages 70-77.*

In recent times, various types of water purification plants have been employed to produce clean water from seawater, as a means to overcome water deficit problems. However, this process results in the production of highly concentrated reject brine solutions, which can cause significant environmental and ecological problems due to their high ionic concentration when released into the near-shore area without treatment. Conversely, these reject brine solutions can be regarded as a promising reactant for providing metal cations during the conversion of CO_2 into inorganic materials, rather than treating them as wastewater. This study proposes a CO_2 -based post-treatment process for desalinated reject brine and investigates the relationship between the ionic concentration of the reject brine solution and the polymorphic properties of inorganic compounds produced by the reaction between metal cations and CO_2 . The polymorphic properties of metal carbonates were investigated with respect to the gradual changes in the concentration of the reject brine solution through dilution and concentration. As a result of this study, the degree of reaction inhibition was found to be based on the concentration of the reject brine solutions, and these results can be applied in multidisciplinary areas, including climate change mitigation, post-treatment of desalinated brine, and advanced materials and resource production.

- **Keywords:** CO_2 utilization; Polymorphic control; Cationic concentration; Brine utilization; Desalinated reject brine

Kevin McSweeney, James Curry, Rick Curtis, Ezra Wari, Weihang Zhu, Brian Craig, Muhammad Muzamil Hussain, Arturo Haces-Garcia, Oghosa P. Idahosa, Emad Zeni, Gubbala Seshasaikrishna. *Development of a comprehensive multi-component toolkit for offshore safety culture assessment.* Pages 78-87.

This paper presents the development of a comprehensive self-assessment safety culture toolkit for the U.S. offshore oil and gas industry. Safety culture impacts organizational safety performance. Measuring safety culture will help an organization better understand the room for safety improvement. The major components of this toolkit are safety culture surveys, interviews, site safety walkthroughs, a review of previous incident investigations, a review of potential leading indicators (accident precursors), and a Safety and Environmental Management System (SEMS) review. This multi-component toolkit is expected to allow a comprehensive assessment of the offshore safety culture at single or multiple facilities. With careful wording of survey questions, safety culture surveys can provide insight into employee perceptions of safety. The paper discusses how safety culture surveys can be incorporated with all other key components to give a more complete picture of an organization's safety culture. A safety maturity model is proposed to incorporate the results from these safety culture measurements to describe an organization's safety maturity level. Like many safety maturity models, the model in this toolkit describes the safety culture maturity in a range from a reaction to events to continual improvement. The analysis of crucial safety culture-related assessment components supports the identification of a safety culture maturity level.

- **Keywords:** Offshore safety culture; Assessment toolkit; Multi-component toolkit; Safety

Youwei Guo, Guoqing Xiao, Jian Chen, Lingyuan Wang, Hongbo Deng, Xiang Liu, Qiang Sun, XingYu Xiong. *Investigation of ambient temperature effects on the characteristics of turbulent diffusion flames: An experimental approach.* Pages 88-98.

Pool fires, commonly associated with industrial accidents, have posed a significant threat to the safety of industrial processes. This is particularly relevant in environments where storage tanks, engine cabinets, and boiler rooms are typically maintained. The effects of ambient temperature on the flame characteristics of gaseous pool fires were explored through a series of experiments conducted in a temperature-controlled chamber, with temperatures ranging from 40 °C to – 20 °C. A modified flame height correlation accounting for the temperature effect was proposed. These findings have potential implications for enhancing the reliability of industrial design and fire risk assessment in environments with varying temperature conditions.

- **Keywords:** Pool fire; Flame height; Ambient temperature; Pulsation frequency

SooHwan Jeong, Jonghun Lim, Seok Il Hong, Soon Chul Kwon, Jae Yun Shim, Yup Yoo, Hyungtae Cho, Sungsu Lim, Junghwan Kim. *A framework for environmental production of textile dyeing process using novel exhaustion-rate meter and multi-layer perceptron-based prediction model.* Pages 99-110.

In textile industries, a lot of wastewater are discharged which are one of the major environmental pollution problems, because they release undesirable dye effluents. Owing to re-dyeing procedures performed to meet customized color specifications, environmental pollution is a serious problem because of the emission of large volumes of wastewater. To solve the environmental problems caused by re-dyeing, the right-first-time (RFT) %, which is the rate at which the target quality is obtained with just one

dyeing, must be increased by considering the dyeing conditions that affect product quality. Here, this study suggests a framework for cleaner production of textile dyeing process using novel exhaustion-rate meter (NERM) and multi-layer perceptron-based prediction model to solve the environmental problems caused by re-dyeing procedure by controlling the exhaustion-rate outliers. The proposed NERM measures the exhaustion-rate based on absorbance of the dyeing solution and is composed of measuring and analysis section. The dyeing solution absorbance is metered in the measuring component through a detector, which performs high-resolution measurement (0.3–1.5 nm full width at half maximum) via a 25- μm slit in the 200–1100-nm wavelength range; the absorbance is then converted to the exhaustion-rate based on Beer's law in the analysis section. Using the NERM, an exhaustion rate dataset according to the Na_2SO_4 and Na_2CO_3 consumption is acquired and a surrogate model that augments the exhaustion rate data is developed. The MLP-based prediction model is then developed using the augmented data to control the real-time exhaustion-rate outliers. As a results, the model performance as regards Na_2SO_4 and Na_2CO_3 prediction is indicated by R^2 values of approximately 0.985 and 0.998, respectively, and root mean squared errors (RMSE) of approximately 1.477 and 1.000, respectively. In addition, the effectiveness of the proposed framework is demonstrated through application to several scenarios in which the real-time exhaustion rate outliers are detected.

- **Keywords:** Textile industry; Re-dyeing; Right-first-time; Exhaustion rate meter; Multi-layer perceptron-based prediction

Shuang Chen, YeJia Lv, Jiaying Hong, Luman Hou, Jia Zhang, Xiaoqiao Zhang, Xiangyu Zhao, Lixin Wang, Guangren Qian. *Recognizing the formation of single-atom vanadium by enthalpy and its advantage in selective catalytic reduction of nitrogen oxide. Pages 111-118.*

Developing a more effective catalyst for the environmental pollutant is always the pursuit of worldwide researchers. In previous reports, most works were focused on prepared catalysts, and more efforts should explore process from a precursor to the formed catalyst. In this work, V supported TiO_2 catalysts were synthesized with different V loadings, and compared in selective catalytic reduction of nitrogen oxide. For the first time, differential scanning calorimetry was used to analyze the forming enthalpy for these catalysts. As a result, turnover frequency (TOF) was decreased from 0.05 to 0.001 s^{-1} when the loading was increased from 0.05 to 15 mol%. At the same time, the forming enthalpy was decreased from 16.53 to 1.80 $\text{KJ}\cdot\text{mol}^{-1}$. Spherical Aberration Corrected Transmission Electron Microscope recognized both single-atom and cluster V even at the lowest loading. What's more, density functional theory revealed that single-atom V had a lower dehydrogenation energy (1.088–1.152 eV) than cluster V during the catalysis (1.834–1.850 eV). According to these evidences, single-atom V had bigger formation enthalpy, lower dehydrogenation energy, and larger TOF than cluster V. These results help to optimize the preparation process for an effective catalyst, which is in favor of hazardous-pollutant treatment.

- **Keywords:** Single atom vanadium; Vanadium cluster; Enthalpy; SCR; Dehydrogenation

Zhengang Lou, Hang Xu, Lijuan Xia, Wenhao Lin, Zhengbo Dai, Xiaonan Wang. *Enhanced freeze-thaw cycles facilitate the antibiotic resistance proliferation and dissemination risk under global climate change. Pages 119-128.*

Antibiotic resistance genes (ARGs) and antibiotic resistant bacteria are considered as emerging contaminants, whose proliferation and dissemination are highly related to the climate conditions. Freeze-thaw cycles (FTC) is a natural phenomena that widely

occurred in terrestrial ecosystem for high latitude environments, and frequent FTC has been revealed under global climate change. However, the effects of FTC on the resistome in soil are still not clear. Thus, a simulation experiment was performed to illustrate the profiles of ARGs and mobile genetic elements (MGEs) under FTC exposure. It was found that, 56.4–73.2% of the shared 71 core ARG subtypes were enriched after FTC treatment, and the abundance of ARGs in total had a significant positive linear correlation with the number of FTC in spite of the declined number of ARG subtypes ($r = 0.986$, $p = 0.002$). This can be explained by the selection pressure exerted by freeze-thaw on bacterial community structure and promoted horizontal gene transfer (HGT). The bacterial classes within phylum Actinobacteria, one of the dominant bacterial phyla accounting for 36–54% of the total bacteria, were enriched because of their spore and filamentous producing attributes, and enormous ARGs were presented in this kind of antibiotic-synthesising bacteria. Moreover, the survived Actinobacteria could serve as ARG donors and receptors, which profit the HGT of ARGs. The present study revealed the facilitation posed by FTC on the proliferation and dissemination of ARGs, and the accordingly findings provide new insights for well understanding of the environmental behaviour of ARGs.

- **Keywords:** Antibiotic resistance genes; Global climate change; Freeze-thaw cycles; Phylum Actinobacteria; Horizontal gene transfer

Jiaxin Zhang, Miao Zhang, Zemin Feng, LV Ruifang, Chenyang Lu, Yiyang Dai, Lichun Dong. *Gated recurrent unit-enhanced deep convolutional neural network for real-time industrial process fault diagnosis. Pages 129-149.*

When deep learning-based models are employed for the fault diagnosis of chemical processes, problems of poor calculation accuracy and efficiency often occur in the scenarios of high-dimensional, nonlinear, and time-varying data, which affects the overall robustness of the fault diagnosis model. This study proposes a novel Gated Recurrent Unit (GRU) - enhanced deep convolutional neural network (EDCNN) model for the improved fault detection and diagnosis of chemical processes. In the GRU-EDCNN model, a maximum smooth function (MSF) is developed and presented to replace the classical activation function for better matching the input data format, which can significantly improve the calculation accuracy and the overall efficiency of DCNN models. Moreover, the convolutional layers in DCNN are optimized by a decentralized convolutional structure, thereby reducing the problem of parameter redundancy. The issue of gradient disappearance is tackled by the embedment of GRU, whose ability to control time series features and gateway information can ensure that no overfitting occurs in the GRU-EDCNN training processes. In two case studies, the GRU-EDCNN model was applied to the benchmark Tennessee Eastman (TE) process and an acid gas absorption process, and the corresponding data of fault diagnosis rate (FDR), false positive rate (FPR), and fault diagnosis time (FDT) of the GRU-EDCNN model were analyzed and compared with those of the other deep learning-based models, verifying the effectiveness of the GRU-EDCNN model for fault diagnosis in both simulated and real-time industrial processes.

- **Keywords:** Gated recurrent unit; Enhanced deep convolutional neural network; Fault diagnosis; Deep learning, maximum smoothing function

Mehmet Ali Topçu. *Production and characterization of zinc oxide nanofibers derived from waste material as precursor. Pages 150-159.*

The emergence of industrial wastes brings with it a series of global environment issues. However, using these wastes including valuable metals as a source of value-added materials will lead to many advantages. The metals can be recovered and transformed for nanomaterial production which offers utility in many applications such as energy conversion and hydrogen evaluation. In this study, recycling techniques were used to

synthesize zinc oxide nanofibers from waste brass flue dust. Initially, characterization and experimental analyses were used to confirm the synthesized nanofibers phase purity, morphology, and optical properties. The X-Ray diffraction (XRD) analysis and X-ray photoelectron spectroscopy (XPS) confirmed the nanofibers produced after recycling process were predominantly ZnO and have high purity. It was determined from scanning electron microscopy (SEM) and transmission electron microscopy (TEM) analysis that the produced samples were in fiber form in nanoscale and high crystallinity. According to the ultraviolet visible spectroscopy (UV-Vis) analysis, the optical band of ZnO nanofibers was found as 3.19 eV. It has been demonstrated with this study that the ZnO nanofibers derived from industrial waste can be used in several energy applications. Also, it was revealed that metal-containing wastes can be disposed of by producing value-added nanomaterials directly from industrial wastes with economical value.

- **Keywords:** Waste recycling; ZnO; Nanofibers; Electrospinning; Characterization

Yin Duan, Xiaobo Liu, Lin Zheng, Zeinab Khalid, Ling Long, Xuguang Jiang. *MgO-based binders with different formulations for solidifying Pb and Cd in MSWI fly ash: Solidification effect and related mechanisms.* Pages 160-167.

The MgO-based binder is a novel and effective material for solidifying municipal solid waste incineration fly ash (MSWI FA). In this study, the effect of MgO-based binders with different MgO contents on the solidification and stabilization of MSWI FA was investigated by adjusting the proportions of MgO, silica fume, and MSWI FA in the solidified system. The leaching behavior and immobilization mechanisms of Cd and Pb in the solidified bodies were focused on. The hydration products generated were characterized by XRD, FTIR, and TG analysis. The results demonstrated that the compressive strength of the solidified bodies and the immobilization efficiencies of heavy metals improved with the increase in MgO addition. The MSWI FA solidified by MgO-based binders could maintain low leaching toxicity over a wider pH range. The generated Mg-containing hydration products, including Mg(OH)₂ and M-C-S-H gels, were believed to contribute to the reduction of the leaching concentrations of heavy metals. The immobilization mechanisms of Pb and Cd were different: the immobilization of Pb came from chemical chelation, and Cd was stabilized from alkaline precipitation. In conclusion, this work provides new insights into applying MgO-based binders in MSWI FA solidification.

- **Keywords:** MSWI fly ash; MgO-based binders; Solidification; Leaching behavior; Hydration products

Le-Duy Nguyen, Myungbae Kim, Yongshik Han, Byungil Choi, Kyuhung Do. *Numerical determination of the required insulation thickness for steel protection against accidental cryogenic exposure.* Pages 168-177.

Cryogenic spill protection by insulation is widely used as one of the most effective risk-mitigation measures to protect steel structures against accidental cryogenic spills. This study proposed, for the first time, a numerical method for predicting the insulation thickness. The method is a combination of an optimization technique and the solution to the heat conduction problem. The major difficulty lies in the boundary condition at the boiling surface, which has not been clearly stated in the literature. To accurately determine the boundary condition, the effect of the insulation thickness on the transient pool boiling heat transfer of a cryogenic liquid on an insulated steel flat plate was first studied. It was determined that the boiling resistance generally decreased with increasing insulation thickness, which suggested that the liquid and boiling surfaces could be assumed to have perfect thermal contact. Subsequently, the assumption of perfect thermal contact was proven to be a valid boundary condition for sufficiently thick insulation layers. The developed method was verified and used to draw the correlations

of the insulation thickness with the period of resistance and metal thickness. The findings of this study are expected to aid in the design of steel structure's cryogenic spill protection systems.

- **Keywords:** Cryogenic spill protection; Passive fire protection; Insulation; Period of resistance; Limiting temperature; Perfect thermal contact

Chee Yung Pang, Gulnaziya Issabayeva, Yean Ling Pang, Mee Chu Wong, Mohamed Kheireddine Aroua. *Derivation and characterization of secondary zinc oxide from rubber glove manufacturing wastewater via adsorption-desorption-precipitation route. Pages 178-189.*

The demand for zinc oxide surged during the Covid-19 pandemic as gloves became a necessity in daily life. The washing-off of the zinc oxide used to activate crosslinking in glove latex, generates hazardous zinc-containing wastewater, which is conventionally treated by chemical precipitation using lime and caustic soda. This produces large volumes of hazardous sludge. This study aims to demonstrate removal and recovery of zinc from real wastewater via adsorption-desorption-chemical precipitation approach to produce utilizable secondary zinc oxide. A low-cost palm shell activated carbon was used to adsorb zinc from raw wastewater with 93% efficiency, straightforwardly reducing zinc concentration below 2 mg/L (discharge standard) within 45 min, at pH 7 and 60 °C. Subsequent desorption with 0.3 M HCl facilitated recovery of 63% of secondary zinc oxide from the desorption solutions via chemical precipitation and calcination path. Morphological analysis of the synthesized secondary zinc oxide confirmed high crystallinity of hexagonal wurtzite crystalline structure of typical spherical and nanorods particle shapes measuring 102 nm in size. Surface area comprised of considerable 59.02 m²/g, with pores volume and size of 0.1735 m³/g and 11.76 nm, respectively. This study demonstrated successful recovery of zinc ions from raw industrial wastewater to produce good quality secondary zinc oxide, creating opportunities for zinc recycling, reduction in consumption of chemicals and chemical sludge volume, steering way towards sustainable practices in rubber gloves manufacturing sector.

- **Keywords:** Adsorption; Palm shell activated carbon; Rubber gloves; Zinc oxide; Zinc oxide synthesis; Zinc recovery

Haowei Yao, Kefeng Lv, Zhen Lou, Mengyang Xing, Hengjie Qin, Huaitao Song, Zhongbin Lv, Dong Wang, Zhenyu Wang, Wei Ren. *Simulation study on oil pressure problems caused by internal faults in oil-immersed transformers. Pages 190-198.*

When internal faults occur in an oil-immersed transformer, the transformer oil inside the cabinet is subjected to thermal decomposition at high temperatures or arcing and produces a mixture of hydrocarbon gases with a risk of vapor explosion. Three-dimensional models of AC 220 kV, AC 500 kV, and DC ± 800 kV oil-immersed transformers were developed for numerical simulations. For these three transformers, the pressure distribution clouds inside the tank and the pressure variation curves at different positions discharge after the occurrence of a short-circuit arc fault between winding turns and at the connection between the tank body and the bushing. It was found that within 50 ms after the fault, the transformer oil vapor expanded rapidly and created a pressure difference at the oil-gas interface. As the oil vapor pressure continued to increase, the pressure inside the tank rose suddenly and transient pressure peaks of varying degrees (up to 0.65 MPa) appeared successively at different locations inside the tank. When the transformer tank pressure limit was exceeded, the tank cracked or exploded easily under uncontrolled conditions.

- **Keywords:** Oil-immersed transformers; Steam explosion; Numerical simulation; Short-circuit arc; Pressure crest

Zengwu Wang, Jintao Gao, Xi Lan, Guoliang Feng, Zhancheng Guo. *An environmental-friendly method for recovery of aluminum droplets from aluminum dross: Mechanical activation and super-gravity separation.* Pages 199-211.

Aluminum dross produced from the smelting process of aluminum is a toxic solid waste that easily hydrolyzes and releases poisonous gases in contact with water, which contains large numbers of fine oxidized aluminum droplets. In this study, an environmental-friendly method for efficient recovery of aluminum droplets from aluminum dross was proposed through mechanical activation and super-gravity separation. Firstly, the aluminum dross with different particle sizes of 8.0–50.0 mm, 4.0–8.0 mm, and < 4.0 mm was mechanically activated, and the oxidized films of metallic aluminum droplets were greatly destructed via milling. However, the driving force of gravity was not sufficient to drive the molten aluminum droplets to detach from the oxidized films at high temperatures. With the enhancement of the super-gravity field, almost all of the aluminum droplets efficiently escaped from the oxidized films and fully recovered from the aluminum dross within 5 min with a high recovery ratio of 97.14% and a high purity of 99.17 wt%. Compared to the conventional process of separating aluminum, this study provides an environmental-friendly method to efficiently recover aluminum droplets from aluminum dross without the problems of secondary aluminum dross production, dust pollution, and gas pollution.

- **Keywords:** Aluminum dross; Aluminum droplets; Mechanical activation; Super-gravity separation; Environmental-friendly

Feng Hong, Huancheng Xue, Xi Yuan, Luyan Wang, Hailin Tian, Liqun Ye, Jinping Jia, Diwen Ying, Yingping Huang. *Numerical investigation on the hydrodynamic performance with special emphasis on the cavitation intensity detection in a Venturi cavitator.* Pages 212-226.

Venturi is one of the structures that have been frequently adopted for the generation of hydrodynamic cavitation, which is now a promising technology and method in wastewater treatment. Despite the wide spread application, insight into the characteristics of cavity dynamics and cavitation intensity to optimize cavitation performance remains lacking. This paper presents computational investigation of the cavitation performance with emphasis on cavitation intensity prediction inside a Venturi cavitator, through a robust modeling approach. Particularly, a new physical model as the criterion to account for the evaluation of cavitation intensity was developed. The predictions gave satisfactory agreement with published data for acoustic bubble dynamics, and experimental results for typical cavitation characteristics of the Venturi. Further investigations analyzed the size oscillations, collapse pressure and collapse temperature of bubbles, as well as the cavitation intensity during its dynamic behavior of the hydrodynamic cavitation in this cavitator. The results showed that the bubbles originally generated near the wall of the Venturi had the strongest oscillations for cavity dynamics. The normalized average bubble collapse pressure was consistent with the distributions of the cavitation intensity within the whole flow domain. Besides, the rear part of the attached cavity at the stage of developing cavitation showed the strongest intensity of cavitation, while the chocking cavitation had no advantage for this issue. This research provides an available and useful criterion to effectively compare and evaluate the bubble dynamics and cavitation intensity in the multiphase flow of cavitational reactors.

- **Keywords:** Venturi cavitator; Hydrodynamic behavior; Cavitation intensity; Bubble dynamics; CFD simulation

Miao Gong, Jinxiang Hu, Qiao Xu, Yujie Fan. *Catalytic gasification of Enteromorpha prolifera for hydrogen production in supercritical water.* Pages 227-237.

This study investigated the effects of the reaction parameters on the supercritical water gasification (SCWG) of *Enteromorpha prolifera* for producing hydrogen-rich syngas and evaluated the hydrogen production performance of four commercial catalysts (KOH, Ni, K₂CO₃, AlCl₃) and their combinations. A higher temperature, a longer reaction time, and an appropriate moisture content were found to contribute to a higher hydrogen yield. The maximum H₂ yield (19.5 mol/kg OM, which was 145 times higher than that without catalyst) was achieved at 400 °C, 30 min, 95% moisture content, and 10 wt% AlCl₃ loading. The catalytic performance of the catalysts followed the order AlCl₃ > KOH > K₂CO₃ > Ni. Due to the limited range of composite ratios explored in this study, the H₂ yield obtained with the combined catalyst was slightly lower compared with that achieved with the individual addition of KOH or AlCl₃. The addition of AlCl₃ could promote biomass decomposition and increase hydrogen production via the steam reforming reaction, while the combination with H₂O₂ also promoted the degradation and gasification of organics, and further increased the total gas yield. The results suggest that AlCl₃-catalyzed SCWG could be a potentially applicable approach for the conversion of *Enteromorpha prolifera* to hydrogen-rich syngas.

- **Keywords:** *Enteromorpha prolifera*; Supercritical water gasification; Hydrogen; Catalysts; AlCl₃

Hang Yao, Lei Ni, Yinshan Liu, Gang Fu, Juncheng Jiang, Zhen Cheng, Yuqing Ni, Zhiquan Chen. *Process hazard and thermal risk evaluation of m-xylene nitration with mixed acid.* Pages 238-250.

The exothermic pattern of m-xylene nitration with mixed acid in semi-batch mode was studied by reaction calorimetry. Adiabatic temperature rise (ΔT_{ad}) and reaction enthalpy (ΔH) were obtained to identify the thermal hazard. Process conditions including stirring rate, reaction temperature and strength of mixed acid were studied to optimize the reaction. Optimal yield (95.5%) was reached under the conditions of sufficient stirring rate, 70% strength of mixed acid and reaction temperature of 40 °C. Meanwhile, the thermal stability of nitration products was investigated by differential scanning calorimetry (DSC) and accelerating rate calorimetry (ARC). Pyrolysis kinetic parameters were calculated under non-isothermal and adiabatic conditions. Furthermore, the maximum temperature of the runaway system for synthesis reaction (MTSR) was determined to analyze the reaction hazard. The thermal risk of nitration of m-xylene was also assessed by the risk matrix and Stoessel criticality diagram. In addition, the nitration mechanism of m-xylene was presented. The active site for the electrophilic reaction of m-xylene was predicted via theoretical approach which was in consistent with the selectivity obtained by the experiment. These findings provide guidance for the safe operation of m-xylene nitration and can be used for further scale-up.

- **Keywords:** Reaction calorimetry; Kinetic parameters; Reaction hazard; Thermal risk; Nitration mechanism

Moshood Onifade, Khadija Omar Said, Amtenge Penda Shivute. *Safe mining operations through technological advancement.* Pages 251-258.

With the introduction of advanced technology, different aspects such as communication, minerals handling and transportation and responses to emergencies, safety, production, and environmental protection in mining operations have improved. Technological advancement has played a very pivotal role in the prevention of mining hazards thereby improving efficiency in the mines. Several technologies have been developed to pave way

for a unified approach for mining operations. The evolution of technology in mining is discussed right from mechanization to automation while addressing the various safety challenges faced in both surface and underground mines. To further appreciate technological advancement in mining, key safety techniques used to promote safety during drilling and blasting, ventilation, underground mine support and slope stability were reported. Despite the enormous contributions that emanate from mining that are crucial for human survival such as the production of building materials and minerals for processing medication, the sector is compelled to adopt better techniques to improve production efficiency and reduce environmental and safety risks to inject sustainability into the whole value chain. Furthermore, the major milestones achieved in improving communication in mining which has been proven to be the most crucial elements needed to promote safety in mining was discussed.

- **Keywords:** Technological advancement; Communication; Mining technology; Mine health and safety

Debasish Tikadar, Ashish M. Gujarathi, Chandan Guria. *Towards retrofitting based multi-criteria analysis of an industrial gas sweetening process: Further insights of CO2 emissions.* Pages 259-271.

Natural gas processing is currently facing economic and environmental challenges due to abrupt changes in oil prices and the development of an alternate source of energy. Therefore it is essential to optimize the processing unit to make it profitable and environmentally friendly. Sustainable optimization of an industrial natural gas treatment plant is carried out using the NSGA-II algorithm for the methyl diethanol amine (MDEA) process to optimize CO₂ removal along with payback period and damage index. This multi-objective optimization study includes seven decision variables such as temperature and pressure of feed gas, feed flow rate, temperature and pressure of regenerator feed, lean amine temperature, and MDEA concentration. Three separate two-objective optimization study problems are developed and applied for retrofitted case and base case studies. Two different ProMax models are developed and validated the model by using actual plant data. All the retrofitted cases and base cases are solved and the Pareto optimal fronts are obtained. Trade-offs between different objectives are illustrated for all the problems. The lean vapor compression process can facilitate maximum H₂S removal of 99.75% and maximum CO₂ removal of 98.52% simultaneously by maintaining a DI value of 476. TOPSIS method is used to rank and find the best optimal solution. Optimization study for uncertain CO₂ concentration (4% mole) in the feed gas is also analyzed and compared with normal feed conditions. The machine learning approach is used to obtain the predictions of selected objective functions for all the problem cases using the decision tree method.

- **Keywords:** Natural gas sweetening; Multi-objective optimization; CO₂ removal; Machine learning; Uncertainty; Pareto ranking

Li Sun, Xianlian Wang, Qingsong Hua, Kwang Y. Lee. *Energy scheduling of a fuel cell based residential cogeneration system using stochastic dynamic programming.* Pages 272-279.

Decarbonization of residential systems is one of the effective ways to achieve the low carbon goal. Due to the advantages of cleanness, efficiency and flexibility, hydrogen fuel cells play a key role in driving the transition to low carbon or carbon-neutral systems. This paper studies the optimal energy scheduling of an off-grid residential cogeneration system composed of a fuel cell, photovoltaic (PV) device, battery, thermal energy storage (TES) and heat pump. With the objective function being fuel cost, the economic optimization scheduling model is developed based on security constraints of devices and power balances of supply and demand. To handle the system uncertainties and achieve global optimality, the stochastic dynamic programming (SDP) algorithm is used, where

the random variables are modeled as time-varying Markov chains. Simulation results under the typical winter day scenarios show that the SDP algorithm can achieve efficient scheduling while enhancing the device sustainability. Besides, comparison results with dynamic programming (DP) in scenarios with different uncertainty degrees demonstrate the optimality and robustness of SDP. Additionally, the impact of TES capacity on the system operation is also discussed, which has certain instructive significance for system capacity configuration in terms of economy and sustainability.

- **Keywords:** Fuel cell; Markov chain; SDP; Energy scheduling; Cogeneration

Ke Liu, Shu Hu, Xiaoqing Wei, Tingting Zuo, Quantong Che. *Accelerating proton conduction in proton exchange membranes with sandwich structure based on carbon nanotubes oxide. Pages 280-289.*

Carbon nanotubes (CNTs) with a high aspect ratio can theoretically realize the concept of channel-like proton transport clusters. In this research, carbon nanotubes oxide (OCNTs) with large amounts of oxygen-containing groups constituted successive proton conduction channels, deriving from the surface oxidation of CNTs. Proton exchange membranes (PEMs) with sandwich structure were constructed through a couple of polyvinyl chloride nanofibers (PNs) mats wrapping a thin OCNTs layer. In the prepared (PNs/OCNTs/PNs)es membrane, the outer polyvinyl chloride (PVC) nanofibers delayed the leakage of the inner OCNTs and enveloped phosphoric acid (PA) molecules. Furthermore, more PA molecules were combined by the oxygen-containing groups of hydroxyl, epoxy and carboxyl on the surface of OCNTs with intermolecular hydrogen bonds. For the (PNs/OCNTs/PNs)es/PA membrane, the good structure stability, high proton conductivity and reinforced mechanical property were derived from the compact structure, fast proton conduction and the formation of inorganic-organic composites. Specifically, the maximum proton conductivity was 4.46×10^{-2} S/cm at 160 °C, higher than 2.75×10^{-3} S/cm of the PVC/OCNTs/PA membrane. Notably, the tensile stress values reached 5.42 MPa of the (PNs/OCNTs/PNs)es membrane and 7.32 MPa of the (PNs/OCNTs/PNs)es/PA membrane. Even after a 350 h non-stop measurement at 120 °C, the (PNs/OCNTs/PNs)es/PA membrane could have the complete surface, albeit with tiny cracks on cross section. The proton conductivity could maintain the proton conductivity of 3.17×10^{-2} S/cm at 160 °C. The research revealed that OCNTs provided the channel-like ionic clusters for proton conduction and sandwich structure accelerated proton conduction in the OCNTs-based membranes.

- **Keywords:** Carbon nanotubes oxide; Electrospinning; Polyvinyl chloride nanofibers; Sandwich structure; Proton conductivity; Proton exchange membranes

Pengqian Wang, Chang'an Wang, Chaowei Wang, Yongbo Du, Defu Che. *Experimental investigation on co-combustion characteristics of semi-coke and coal: Insight into synergy and blending method. Pages 290-302.*

Co-combustion of semi-coke and coal is a prospective technique for large-scale disposal or utilization of the solid waste. In this paper, the co-combustion behaviors and kinetics of semi-coke and coal were studied by thermogravimetric analysis with a focus on the influence of blending method and synergy. The results indicated that the semi-coke combustion was improved by blending with coal, and the interaction between fuels tended to promote the co-combustion. The ignition and burnout temperatures were positively correlated with the carbon content of the mixture, while the comprehensive combustion index and stability index were negatively correlated with it. The layer blending and partition blending method seemed to show stronger promotion than uniform blending method, and the layer blending method with coal in the upper layer was recommended due to the better combustion behavior. The promotion of coal on semi-

coke combustion was less affected in devolatilization stage but weakened by the decrease of O₂ concentration in char burnout stage. The apparent activation energy (E_a) of the mixture decreased with the increasing fraction of coal. The layer blending method with coal in the upper layer had the lowest E_a in devolatilization stage and relatively high E_a in char burnout stage. The work can give some new insights into waste co-disposal strategy and carbon emission reduction in China.

- **Keywords:** Solid waste; Co-combustion; Synergy; Blending method; Kinetics

Bing Zhao, Xiangyan Kong, Yongsheng Sun, Yuexin Han, Yanjun Li. *Novel metallic Fe recovery from copper smelting slag by the deep reduction method with renewable biochar reducing agent: Phase transformation process and Fe particle growth optimization.* Pages 303-318.

The land stockpiling of copper smelting slag causes serious environmental pollution and resource waste. It contains a large amount of Fe, which is difficult to recover by traditional methods. In this paper, a novel metallic Fe recovery method was presented by deep reduction with renewable biochar as a reducing agent. It not only recovers metallic Fe but also relieves the pressure of iron ore with a sustainable and eco-friendly method. It was found that the metallization ratio variation trend was explored by the temperature, time, CaO content and C/O molar ratio increasing. When biochar was used as a reducing agent, the metallization ratios of Fe under different reduction conditions were better than the traditional reducing agent coal, which indicated that biochar could replace coal as a reducing agent. The phase transition and microstructure change during the deep reduction process were analyzed by XRD, XPS and SEM-EDS. The metallic Fe particles were formed from the copper smelting slag particle outside and spread to the inside gradually, distinguishing the slag phase and metal phase eventually. The growth kinetic equations of the two stages were obtained after calculation and simulation. There's a certain amount of truth to the predicted value because R² is 0.9745 with experimental measurements. This study demonstrates that the deep reduction is a green and effective technology for copper smelting slag utilization.

- **Keywords:** Copper smelting slag; Renewable biochar; Metallic Fe recovery; Phase transition; Microstructure change

Ashkan Tizvir, Mohammad Hassan Shojaee fard, Gholam Reza Molaeimanesh, Ali Reza Zahedi, Sina Labbafi. *Optimization of biodiesel production from microalgae and investigation of exhaust emissions and engine performance for biodiesel blended.* Pages 319-340.

This paper evaluates the potential of using biodiesel from *Dunaliella tertiolecta* in the internal combustion engine to reduce emissions and fuel consumption and increase power output. The high cost of microalgae biomass production, the low efficiency of converting biomass into biodiesel and the increase in NO_x production and fuel consumption with the combination of biodiesel in high percentages are the problems of this issue. In this article, by using the new solar still desalination/parabolic trough collector/geothermal hybrid system to supply the required water and heat and to investigate the effect of the influencing factors, the efficiency of microalgae production and transesterification process's conversion efficiency were obtained as 1.04 g/L and 80.22%, respectively. The addition of biodiesel from 0% to 20% in the fuel decreased CO, SO_x and HC emissions, but CO₂ and NO_x emissions increased. Also, fuel consumption increased and engine output power decreased. The optimum point was found in order to emit the least emissions and reduce fuel consumption and increase the output power for the composition percentage of 11.5% biodiesel in the fuel.

- **Keywords:** Biodiesel; Renewable energy systems; Microalgae; Engine performance; Transesterification

Xuezhou Fan, Hazim Moria, Shaker A. Reda, Fayez Aldawi, Nguyen Truong, Shuwen Wu. *Geothermal assisted Rankine cycle for performance enhancement of a biomass-driven power plant; Thermoeconomic and environmental impact assessment.* Pages 341-354.

In view of the environmental concerns of increasing fossil fuel consumption, the renewable energy sources are promising alternatives, among which the biomass and geothermal energies are the two most common and mature ones. In the present research, a novel Electricity Generation System (EGS) driven by hybrid biomass fuel and geothermal source is developed and its performance is compared with Typical EGS (TEGS) driven by only the biomass fuel. The TEGS consists of a gas turbine cycle and a steam Rankine cycle equipped with an open-feed water heater (OFWH). In the proposed Hybrid Electricity Generation System (HEGS), the geothermal energy is deployed to heat the feedwater before entering the OFWH, as a result the bottoming Rankine cycle yields more electricity. However, a comprehensive investigation from technical and economic standpoints is required to compare its performance with the relevant TEGS. Therefore, through the application of thermodynamic, thermoeconomic, and environmental methodologies, the considered EGSs performance are modeled and comprehensively analyzed. Based on the modeling results, the maximum exergetic efficiency for the TEGS and HEGS is achieved, respectively as 40.8% and 43.05% under the gas turbine inlet temperature of 1550 K. Final optimal operating conditions are determined through a multi-criteria optimization respect to exergetic efficiency and cost criteria. Under these working conditions, the LCOE and exergetic efficiency for the TEGS are calculated to be respectively as 71.22 \$/MWh and 43.22%. At this point, net electricity, total exergy destruction rate, and CO₂ emission rate are estimated to be as 7750 kW, 9446 kW, and 0.7401 kg/kWh, respectively.

- **Keywords:** Comparative study; Electricity generation system; Environmental effects; Hybrid renewable energy; Thermoeconomic

Yuan Lu, Jamison Chang. *Implementing and maintaining an evergreen risk screening program in an exploration and production company.* Pages 355-360.

A risk screening program has been developed to identify facilities that have the potential impact to public and environmental receptors. This allows the company to assess and effectively manage the risks associated with these facilities through their internal "Specialized Field Risk Management" (SFRM) program. Conducting risk screening and keeping it current in an operating environment is very challenging because of the large number of ongoing development projects, the frequent changes of operating conditions, and public encroachment on these facilities. This paper presents a systematic approach to implement and keep this risk screening program evergreen under these changing conditions. In this approach, existing project management systems such as Management of Change and Well Execution Planner were leveraged to develop and convey the risk screening workflow. In areas of concern such as public encroachment, where monitoring processes were not in place, a risk screening workflow was created to address the gap. This risk screening workflow was also integrated into asset acquisition due diligence activities to support these important business decisions. These workflows were consolidated into a single robust risk screening program managed by a centralized functional group. This program has been proven effective in identifying and avoiding potential high offsite risks in the planning stage of a project, as well as to help manage these risks through the asset's life cycle.

- **Keywords:** Risk management; Risk screening; Management of Change; Offsite risk; Workflow; Life cycle

Jun-Wei Wang, Hamidreza Abadikhah, Liang-Jun Yin, Xian Jian, Xin Xu. *Multilevel hierarchical super-hydrophobic ceramic membrane for water-in-oil emulsion separation. Pages 361-368.*

Hierarchical silicon nitride (Si₃N₄) membranes were fabricated by catalytic growth of α-Si₃N₄ nanowires onto the rod-like β-Si₃N₄ grains. Compared to the bare asymmetric structure of β-Si₃N₄ membranes, the average pore size reduced from 0.9 μm to 0.67 μm, while the porosity decreased slightly from 47 ± 0.6% to 45.3 ± 1.1%. Inorganic nanoparticles derived from organosilane were used to further modify the membranes. The membranes displayed super-hydrophobic characteristics with a water contact angle of 155 ± 1° due to the multilevel hierarchical structure and the -Si-CH₃ low energy terminal groups. The super-hydrophobic membranes were successfully applied for the water-in-oil emulsion separation process. At various driving pressures, the water rejection of the water-in-oil emulsion was higher than 95%. This work's durable super-hydrophobic ceramic membrane has promise for the purification of a variety of oil products.

- **Keywords:** Silicon nitride membrane; Multilevel hierarchical structure; Super-hydrophobic modification; Water-in-oil emulsion separation

Vijaykumar Sekar, Baranidharan Sundaram. *Preliminary evidence of microplastics in landfill leachate, Hyderabad, India. Pages 369-376.*

In recent years, Microplastics (MPs) have gained significant attention all over the world due to their propensity to pollute the environment and transfer toxins into the food chain, thereby endangering human health. Landfill leachate seems to be an obvious source of MPs and has the capacity to contaminate surface water, groundwater and soil. MP pollution in aquatic ecosystems has received significant research attention, whereas MP pollution in terrestrial ecosystems has received less focus. The main objective of this research is to presents the current level of knowledge about the origin, detection, occurrence, and effects of MPs in Indian landfill leachate. MP concentrations in landfill leachate was ranged between 9 and 21 items/L. The most common MP shape was fiber (83%), followed by fragment (11%), film (3%), and foam (2%). The MP colour found in leachate was yellow (35%), transparent (16%), purple (15%), blue (11%), pink (8%), white (6%), black (3%), green (2%), and orange (1%). From the chemical analysis the predominant polymers detected were LDPE, PP, PET, CA, and Nitrile. This study provides information on the properties and quantity of MPs in landfill leachate, launching additional investigation into the mechanisms through which MP s reach the environment.

- **Keywords:** Microplastics; Landfill; Leachate; Waste management; India; Plastic waste

Man-Wen Tian, Zubairu Abubakar, Bhupendra Singh Chauhan, Saleh Mahmoud, Chuang Lui, Ibrahim B. Mansir. *Economic cost and performance analysis of a novel trigeneration scheme utilizing CO₂ capture and solid oxide electrolysis units. Pages 377-391.*

A novel integrated process is presented for power, hydrogen, and heat generation through water electrolysis in the presence of carbon dioxide (CO₂) captured from a power plant flue gas. The proposed system consists of a CO₂ capture unit, a solid oxide electrolysis unit (SOEU), a steam power cycle, a heat recovery unit (HRU), and an ammonia power cycle. The overall energy and exergy efficiencies of the power plant are 34.84% and 83%, respectively. In addition, it is demonstrated that the total exergy

destruction and exergy destruction rate of the proposed cycle are 1357576 kW and 0.081 GJ/kWh. The total net output power of the proposed power plant is determined at 60046.6 kW. Heat recovery values in SOEU and CCU units respectively equal 1158 and 22.17 MW. Based on the exergy analysis, the largest exergy destruction happens in the HRU unit (79%) with a value of 1066340 kW. The environmental analysis indicates that the direct CO₂ emission rate is zero and the indirect one is 0.53 kgCO₂/kWh. Meanwhile, the economic analysis shows that the total annual cost of the proposed power plant is 75.36 M\$ and the production cost of electricity equals 0.15 \$/kW.

- **Keywords:** Flue gas; CO₂ capture; Solid oxide electrolysis; 4E analysis; Renewable power plant

Ke-Yu Chen, Yu-Zhu Huang, Jian-Xiao Wang, Yun-Xia Hu, Xin-Hua Xu, Li-Hua Cheng. *Bidirectional diffusion of functional draw solutions in an osmotic photobioreactor coupling wastewater treatment and microalgal growth*. Pages 392-401.

The osmotic photobioreactor (OsPBR) technology has shown great potential by integrating forward osmosis with algal wastewater treatment. However, the reverse salt flux remains a key challenge. In order to reveal the diffusion behaviors and the transport mechanisms of reverse salt flux (RSF) in an OsPBR, the NH₄HCO₃ and (NH₄)₂HPO₄ (DAP) were compared as draw solutions. The results showed that the biomass growth in OsPBR with NH₄HCO₃ as draw solution was higher than that of DAP initially, reached up to 0.78 g L⁻¹. Although the reverse salt flux of NH₄HCO₃ was twice higher than that of DAP, the OsPBR using NH₄HCO₃ as draw solution exhibited better N & P removal rate than that of DAP, reached at 75% and 100%, respectively. A higher diffusion of cation to anion was further found for DAP as draw solution. This work showed the feasibility to use NH₄HCO₃ as draw solution in OsPBR, which allows the upgrade of microalgal osmotic photobioreactor technology not only in water treatment but also its carbon neutralization potential.

- **Keywords:** Microalgae; Forward osmosis; Reverse solute flux; Wastewater treatment; Ion transport

Yongkui Li, Xiaodong Pan, Suqin Li, Penghui Guo, Xuefeng Gao. *Separation of iron from converter dust by superconducting HGMS: A simulation analysis and experimental study*. Pages 402-413.

Converter dust (LT dust) is an important solid waste from steelmaking, in which iron oxides are the preferred raw material for preparing high value-added α -Fe₂O₃. Since LT dust contains many impurities, the iron oxides in the LT dust must be enriched and purified before the preparation of α -Fe₂O₃. Particle trapping behaviors of the matrices as well as the magnetic flocculation of LT dust particles in superconducting high gradient magnetic separation (S-HGMS) were investigated with numerical simulations and experiments. The geometric shape, aspect ratio a:b, and angle α between the axis and the magnetic field direction of the matrices affected the maximum magnetic field intensity (H_{max}) and effective capture area (Seca). Diamond matrices had better particle-capture capacity than elliptic and circular matrices because the diamond matrices produced a tip effect and increased the magnetic field force. When the cross section of the matrices was parallel to the direction of the particle velocity, magnetic/weakly magnetic particles were more easily captured by the upper and lower ends of the matrices compared with that of two sides because the particle velocity at the upper and lower ends of the matrices was smaller than that of two sides, making the magnetic force greater than the drag force. Fe₂MgO₄ and Fe₂O₃ particles were more prone to magnetic flocculation than other particles because of their higher magnetic susceptibility. The dispersant changed the pH of the solution and the charges on the surface of LT dust

particles, and the particles were effectively dispersed because of the action of electrostatic forces. When the magnetic induction was 1.8 T, the dispersant dosage was 20 mg/L, the pulp concentration was 1.5%, and the total Fe content increased by 8.72%, corresponding to an Fe recovery of 91.65%. Finally, a method was developed for extracting iron oxides from LT dust using S-HGMS, to prepare high value-added α -Fe₂O₃.

- **Keywords:** LT dust; Superconducting high gradient magnetic separation; Numerical simulation; Matrices; Magnetic agglomeration

Alexandros G. Venetsanos, Aobo Liu, Michael A. Delichatsios, Yiannis A. Levendis. *Experiments and modelling of liquid nitrogen jet release and dispersion for fire-related applications. Pages 414-425.*

Cryogenic liquid nitrogen (LN₂) is proposed as an effective fire suppressant/extinguisher for challenging fires. Upon reaching a fire source, this inert cryogen vaporizes expediently and separates the fuel from the air. Additionally, it cools the burning fuel and slows down its pyrolysis/gasification reactions. A prior investigation concentrated on the survivability of single LN₂ droplets, following breakup of the jet exiting the nozzle, and the predicted the droplet size that reaches a target. This investigation addresses the application of a liquid nitrogen jet for the extinction of fires with a combination of experiments and theoretical analysis. Small scale laboratory experiments were conducted with a sprayer and larger scale experiments were conducted with a cryogenic hose and nozzle. In these experiments the reach of the liquid nitrogen jets was measured, and their fire extinction capabilities were assessed. Numerical simulations were performed with the ADREA-HF CFD code using the mixture approach and explicit modelling of LN₂ evaporation using the Lee model. Numerical results on the reach of a liquid nitrogen jet qualitatively matched the experimental observations for release of a liquid nitrogen jet in open atmosphere. The Lee model coefficient was found to depend strongly on the nozzle diameter. An integral model was also constructed to explore the effects of relevant parameters, such as the LN₂ storage tank pressure, the initial jet vapor quality, the jet velocity at the nozzle exit and the effects of the ambient air entrainment. Based on experiments and theoretical analysis, it became evident that for effective extinction of a fire with liquid nitrogen a commercial nozzle should have a large diameter and should be brought close to the burning target, i.e., within a few meters. As this action can pose potential safety risks to firefighters, the advancement of the nozzle towards the fire should be operated remotely.

- **Keywords:** Liquid nitrogen jets; Fire suppression; Firefighter safety; HEM; Explicit vaporization rate; Lee model; ADREA-HF code

Zhixiang Xu, Dimeng Zhao, Xianyao Zheng, Kemeng Sheng, Yu Luo, Bo Chen, Bin Huang, Xiaoxia Yang, Xuejun Pan. *The ecotoxicity of single-layer molybdenum disulfide nanosheets on freshwater microalgae *Selenastrum capricornutum*. Pages 426-436.*

Molybdenum disulfide (MoS₂) nanomaterials have attracted considerable attention due to their unique physicochemical properties and promising applications, and subsequent risks to the environment and human health. However, the toxicological investigations of MoS₂ nanosheets in aquatic environments are still limited. Herein, their aquatic toxic effects and involved mechanisms were explored using a freshwater green microalgae model, *Selenastrum capricornutum*. Several endpoints, including algal growth, photosynthetic pigment and macromolecular substances synthesis, were investigated after exposure to 0.02–50.0 mg/L MoS₂ nanosheets. Furthermore, oxidative stress, membrane damage, lipid oxidation, and secretion of extracellular polymeric substances were elucidated as well. The results showed that single-layer MoS₂ (SLMoS₂) nanosheets at low concentrations (\leq 1.0 mg/L) stimulated the synthesis of chlorophyll and primary

macromolecules, and they slightly promoted the growth of *S. capricornutum*. In contrast, higher concentrations of SLMoS₂ (> 1.0 mg/L) inhibited algae growth through ROS-mediated membrane destruction and oxidative damage. Surprisingly, SLMoS₂ accelerated extracellular polymeric substances (EPS) secretion and changed their fluorescent components, thus influencing algal growth. Taken together, MoS₂ nanomaterials exerted bidirectional effects on *S. capricornutum* at the cellular, histological and organismal levels. These results provide considerable support regarding the adverse effects of MoS₂ nanomaterials on freshwater microalgae.

- **Keywords:** Molybdenum disulfide nanosheets; Freshwater microalgae; Ecotoxicity; Dual dose responses; Oxidative stress; Extracellular polymeric substances

Lejia Sun, Chenghao Jia, Yang Miao. *Visualization of hydrogen leak for electro-hydrogen coupled system based on Background Oriented Schlieren*. Pages 437-446.

As the world's energy demand continues to grow and the environmental pollution problem caused by fossil energy sources becomes more and more serious, the hydrogen-electric coupling system is considered a highly competitive new energy supply method in the future. A unique Background Oriented Schlieren (BOS) technique is proposed to detect hydrogen leakage in the low and high power consumption peaks. Firstly, the principle of the BOS is analyzed, and a new inverse function of gas jet concentration distribution is proposed; secondly, a BOS optical experiment system is built, and the displacements of background particles at $z = 10d$, $20d$ and $30d$ at three axial positions are obtained, and the formed undesirable displacement function is corrected by laser beam profile deformation technique, and the radial concentration distribution curves at three axial positions are obtained by concentration inversion. Comparing the concentration distribution curves obtained after the correction with those obtained from CFD simulation and uncorrected BOS experiments, it was found that after the correction, the concentration distribution curves of BOS were closer to the simulation results and could reflect the radial concentration distribution of hydrogen more accurately. We also find that the average expansion angle of the hydrogen jet is about 23° for different combinations of outlet pressure and tube diameter, which is very similar to the theoretical and experimental studies. The hydrogen monitoring system based on BOS technology is a simple device with low cost, high sensitivity, fast response, and high reliability, which provides a new idea and method for hydrogen leak monitoring in a hydrogen-electric coupled system.

- **Keywords:** Hydrogen-electric coupling; Safety monitoring; BOS; Hydrogen leak

Shuaiyong Li, Zhengxu Dai, Mengqian Cai, Liang Liu, Lin Mei. *A novel DVAPSO-LSTSVM classifier in compressed sensing domain for intelligent pipeline leakage diagnosis*. Pages 447-460.

Leakage diagnosis is of great significance for maintaining the normal operation of pipelines. However, there is a large amount of redundant data in leakage data collection, resulting in increased detection time. In addition, the leakage detection model lacks the necessary optimization, which limits diagnostic accuracy. To overcome these two drawbacks, this paper proposes a novel leakage diagnosis model in compressed sensing (CS) domain. Firstly, the leakage signal is converted into the CS domain to reduce redundant data, and extract features in the CS domain to form a feature dataset. Then, a particle swarm optimization algorithm with decreased and variable amplitude strategy (DVAPSO) is proposed, which enhances the ability of particle optimization and jumping out of local optimum. The diagnosis model LSTSVM is optimized using DVAPSO algorithm to decrease the risk of trapping into local optimum in the training process. Finally, the leakage feature dataset of CS domain is sent to the DVAPSO-LSTSVM diagnosis model to

complete the leakage detection. The experimental results show that pipeline data in CS domain improves detection velocity by 71.7% when the compression ratio is 50%. Moreover, the DVAPSO-LSTSVM has higher leakage identification accuracy compared to other diagnosis models, with a detection accuracy of 95.2%.

- **Keywords:** Compressed sensing; LSTSVM; Decreased amplitude strategy; PSO; Leakage diagnosis

Wei Zhang, Heng Li, Siqiang Xiao, Jianfei Wu, Chuanhu Wang, Xiaobin Liu, Qingbiao Li, Yanmei Zheng. *Regulating the electrokinetic delivery of Tween 80 and persulfate for remediating low-permeability phenanthrene contaminated soil: Importance of reducing unproductive consumption. Pages 461-472.*

Controllable delivery of persulfate (PS) and the enhancement of oxidative availability of pollutants in in-situ oxidative remediation of low-permeability polycyclic aromatic hydrocarbons (PAHs) contaminated soil are crucial. To tackle the above challenges, the coupling of Tween 80 solubilization enhanced oxidation of phenanthrene (PHE) in low-permeability soil under electrokinetic remediation (EKR) was proposed. Firstly, batch degradation experiments showed that the addition of Tween 80 significantly inhibited the degradation of PHE in soil under thermally activated PS, as the dosage of Tween 80 increased from 0 % to 1 % with the corresponding removal rate declining from 99.19 % to 40.90 %. Accordingly, in-situ electrokinetic delivery of Tween 80 and PS was regulated in further EKR, intending to reduce unproductive consumption. PS was more uniformly delivered to the whole remediation regions from the cathode chamber by electromigration, while Tween 80 was transported into the soil from the anode chamber by electroosmosis, which made Tween 80 solubilization and PS oxidation achieve synergistic effect. And the total removal rate of PHE reached 64.90 % under this strategy, which had increased by 415.90 % and 8.76 %– 130.14 % compared with only EKR or EKR coupling single enhanced technology, respectively. After further thermal activation of transported PS at 50 °C by electrical resistance heating, the total removal rate of PHE increased to 71.58 %. EPR spectrum indicated that SO₄⁻ and OH[•] were responsible for the degradation of PHE.

- **Keywords:** Electrokinetic remediation; Persulfate; Tween 80; Low-permeability contaminated soil; Phenanthrene; Unproductive consumption

Iman Salahshoori, Majid Namayandeh Jorabchi, Somayeh Ghasemi, Arash Ranjbarzadeh-Dibazar, Mohammad Vahedi, Hossein Ali Khonakdar. *MIL-53 (Al) nanostructure for non-steroidal anti-inflammatory drug adsorption in wastewater treatment: Molecular simulation and experimental insights. Pages 473-494.*

Pharmaceuticals are prevalent in the environment, especially the nanostructures of non-steroidal anti-inflammatory drugs (NSAIDs) in water, which can harm human health and the environment. Adsorption processes are effective and energy efficient for removing contaminants. In this study, a new adsorbent, MIL-53 (Al), was used to remove pharmaceutical pollutants, including diclofenac (DIC), ketoprofen (KET), indomethacin (IND), and mefenamic acid (MFA), from wastewater. This study employed a combination of quantum mechanical (QM) calculations, Monte Carlo (MC) simulations, and molecular dynamics (MD) simulations to understand the adsorption behaviors of these contaminants. This study first analyzed the structures of the contaminants and the adsorbent using various techniques, such as electrostatic potential, reduced density gradients, and Hirshfeld surfaces. Then, we investigated the adsorption affinity of pharmaceutical pollutants on MIL-53 (Al) using the COSMO sigma profile and HOMO–LUMO energies. The simulation results revealed that HBs, electrostatic interactions, and

n-n stacking primarily contribute to the adsorption mechanism. Laboratory tests confirmed the synthesis of MIL-53 using Fourier transform infrared spectroscopy (FTIR), scanning electron microscopy (SEM), energy-dispersive X-ray spectroscopy (EDX), and wide-angle X-ray diffraction (WAXD). Ultraviolet-visible (UV-Vis) spectroscopy was performed to analyze the adsorption of the targeted drugs, and the experimental results agreed well with the modeling results. This study concluded that MIL-53 (Al) has the potential to serve as an effective adsorbent for the removal of pharmaceutical pollutants from wastewater because of its strong adsorption properties.

- **Keywords:** Computational analysis, Metal-organic framework MIL-53 (Al); Molecular simulations; Non-steroidal anti-inflammatory drugs (NSAIDs); Pharmaceutical pollutant adsorption, Wastewater treatment

Wei Zhang, Lei Zhang, Feng Chen, Jie Cai, Yi Liu, JinLing Zhang, XunMing Wang, Madni Sohail. *Multi-objective optimization and exergoeconomic analysis of solar and geothermal-based power and cooling system using zeotropic mixtures as the working fluid. Pages 495-515.*

The current paper proposes a double-flash geothermal system with a dual-pressure organic Rankine cycle binary system. To improve the system's performance, the inlet geofluid is preheated via an indirect mode of a solar system, and an Ejector Refrigeration Cycle system is installed to the geofluid's brine line to produce cooling capacity. Comprehensive investigations are performed to select the Dual-pressure Organic Rankine Cycle's working fluid among various pure substances and zeotropic mixtures that refer to choosing the R245ca/R142b. The system presents 12.12 MW net power at the base mode with a 1.87 MW cooling load and 4.88 years payback period. Some main parameters' change effect on the system is studied. The low-pressure steam turbine's exit pressure influences the cooling load and energetic efficiency. The high-pressure turbine's input pressure affects the total exergy destruction and net power higher than the other. The optimum state of the system is obtained through two energy-economic and exergy-economic assessments. The energy-economic assessment provides a higher cooling load of about 5.7 MW and a lower net power of about 10.8 MW with 4.59 years payback period. The exergy-economic assessment represents 12.22 MW net power and a cooling load of about 1.97 MW with 4.77 years payback period.

- **Keywords:** Parabolic Through Solar Collector; Zeotropic mixture; Energy-economic assessment; Exergy-economic assessment; Multi-objective optimization

Ammar Al Helal, Sarah Ajjaoui, Malik M. Mohammed, Ahmed Barificani, Hussein Znad. *Enhancing oxygen scavenging properties of erythorbic acid through transition metal catalysis. Pages 516-523.*

The presence of oxygen in pipelines used in power plants and the oil industry requires vigilant attention and utilization of oxygen scavenging to prevent the deleterious effects of corrosion. This study aims to investigate the efficacy of four transition metal catalysts (manganese, copper, nickel, and chromium) on the effectiveness of erythorbic acid as an oxygen scavenger. The experimental approach involved injecting varying concentrations (5 ppm, 10 ppm, and 20 ppm) of transition metal catalyst solutions with erythorbic acid at concentrations of 20 ppm, 50 ppm, and 100 ppm, while maintaining a controlled temperature of 25 °C and a pH of 9.0 at a saturated oxygen concentration. The outcome of the study demonstrated that nickel and chromium did not improve the oxygen removal rate, while copper exhibited notable results compared to the control catalyst (manganese). Specifically, the copper (I) chloride solution proved to be the most efficient in reducing dissolved oxygen content to levels below 20 ppb.

- **Keywords:** Transition metal catalysts; Erythorbic acid; Oxygen scavenger

Gongquan Wang, Ping Ping, Yue Zhang, Hengle Zhao, Hongpeng Lv, Xinzeng Gao, Wei Gao, Depeng Kong. *Modeling thermal runaway propagation of lithium-ion batteries under impacts of ceiling jet fire.* Pages 524-540.

Thermal runaway (TR) of lithium-ion batteries (LIBs) is always accompanied by the emission of combustible gases and the resulting jet fire may promote TR propagation in the battery module. An accurate TR propagation model incorporating jet fire provides insights into the cell-to-cell failure mechanism and aids the safety-optimal design of battery pack. In this work, a modeling framework based on conjugate heat transfer is developed to explore the interaction between jet fire and propagation behavior during TR. The LIBs are modelled by integrating chemical reactions, gas generation and jet dynamics, while the jet fire outside the cells is simulated by the CFD models involving combustion. The heat balance is employed to address TR propagation, which fully considers the energy flows between various elements of battery pack. The proposed model is capable of capturing the flame morphology and temperature evolution of cells, fire and ceiling plate, as confirmed by the TR propagation experiment under ceilings. Simulation results demonstrate that increasing the space confinement degrees shortens the propagation time interval by enhancing the convection from ejected gases and the radiation from flame. The reduction of ceiling height extends the flame extension length and significantly accelerates the cell-to-cell failure, highlighting the impacts of jet fire on TR propagation. This work presents a more realistic model for TR propagation, which can provide a pragmatic guidance for the battery pack's fire protection design and process safety assurance in the practical application.

- **Keywords:** Lithium-ion battery; Thermal runaway propagation; Jet fire; Ceiling; Numerical simulation

Umair Baig, M.F. Al-Kuhaili, M.A. Dastageer. *Photo-responsive Zinc Oxide-coated alumina ceramic membrane with super-wettable and self-cleaning features fabricated by single step RF magnetron sputtering for oily water treatment.* Pages 541-553.

Zinc Oxide (ZnO) coated alumina ceramic membrane with super-wettable and photo-responsive self-cleaning features was fabricated by radio frequency (RF) magnetic sputtering, and used as a filtering medium in the dead-end filtration system for oily water treatment. The chemistry of the material in conjunction with the optimum surface roughness accomplish by RF magnetic sputtering rendered a unique surface wettability, favorable for water passing oil-in-water emulsion separation. The second desirable functionality of the membrane is its self-cleaning potential under light irradiation, owing to the efficient photo-catalytic property of ZnO. Oil-surface-air and water-surface-air interfacial contact angles for the membrane surface were measured using goniometer and they are close to 0° (superhydrophilic / superoleophilic in air), whereas under the water oil-surface-water interfacial contact angle switched to 158.70° (underwater superoleophobic). The oil-in-water emulsion separation efficiency, the water permeate flux were measured at different trans-membrane pressures, and oil concentrations in oily water emulsion, and the results showed that 99.9% oil-in-water emulsion separation efficiency was maintained for a range of trans-membrane pressure, and oil concentration for a long duration of use. The highest permeate flux rate and separation efficiency (%) of the fabricated Zinc oxide-coated alumina ceramic membrane were found to be ~ 325 L/m².h and 99.9%, respectively at 2 bar using surfactant stabilized oil-in-water emulsions as feed. However, the water flux declined with reduced trans-membrane pressure, increased oil concentration and with the long use of the membrane. The advantage of ZnO-coated alumina ceramic membrane is that it is water passing, and hence the oil clogging of the membrane is quite minimal. However, with the long use the membrane is prone to the deposition of oily contaminant on the membrane surface,

which resulted in low water permeate flux, and this problem was resolved, and the original permeate flux was restored by routine self-cleaning of the membrane surface by illuminating light on the photo-catalytic ZnO film on the membrane surface. In addition to the wettability studies of the membrane, the structural, chemical and morphological characterizations of the material, and the coated membrane were carried out.

- **Keywords:** Ceramic membrane; ZnO-coating; RF Magnetron sputtering; Super-wettability; Oil-in-water emulsion separation, Photo-catalytic self-cleaning

Zhe Wang, Yudong Liu, Long Meng, Jingkui Qu, Zhancheng Guo. *Extraction of precious metals by synergetic smelting of spent automotive catalysts and waste printed circuit boards. Pages 554-564.*

Spent automotive catalysts (SACs) and waste printed circuit boards (WPCBs) are the most important secondary resource containing precious metals (PMs). A resource-saving process of extracting PMs from SACs and WPCBs by synergistic smelting of these two wastes was proposed. The main feature of the process was to use metal components in WPCBs as the collector metal of PMs and use carrier components in SACs as the slag formative. A SiO₂-FeO-Al₂O₃-MgO-CaO slag system was first designed for the synergistic smelting by analyzing phase diagrams and liquid phase formation. On this basis, the laboratory -scale synergistic smelting experiments of these two wastes were carried out. Under the optimal conditions of 1350 °C, FeO/SiO₂ mass ratio = 1.0, WPCBs/SACs mass ratio = 0.25, 5 wt% CaO content in the slag, and 3 h smelting time, the extraction efficiencies of Pd, Rh, Ag and Au were 90.5%, 93.2%, 98.9% and 94.5%, respectively. In the collected crude Cu ingot after synergistic smelting, PMs were mainly concentrated in the Cu-Sn phase. Also, a potential industrial system for the synergistic-smelting process based on a top-blown injection smelting furnace was proposed. The novel process will provide an effective way for extracting PMs from secondary resources.

- **Keywords:** Precious metals; Waste printed circuit boards; Spent automotive catalysts; Synergistic smelting; Extraction

Nawei Lyu, Shuang Shi, Hongfei Lu, Yuhang Song, Xin Jiang, Yang Jin. *Hydrogen gas diffusion behavior under fault conditions and detector installation optimization of electric vehicles. Pages 565-574.*

The thermal runaway of lithium-ion batteries presents a significant threat to electric vehicles by elevating the risk of fires or explosions. Safety warnings based on special gases such as H₂ and CO are crucial to avoid thermal runaway. However, few studies or applications regarding gas warnings in electric vehicles have been reported. In this study, H₂ detection experiments were performed in a real electric vehicle battery pack, and the H₂ diffusion behavior was studied. The results showed that H₂ can effectively warn about battery faults. In damaged batteries, H₂ may be released from the micro-cracks in the battery or the vent. While H₂ was detected and the power supply was cut off, the cell surface temperature tended to decrease and thermal runaway did not occur. The installation of the detector affects the detection time. Thus, H₂ diffusion simulations starting from different locations were performed, and the installation location was optimized. The results indicated that setting two detectors was optimal, and the optimized detection time (from release to detection of H₂) was 60 s shorter than that before optimization. The experimental and simulation results provide an effective method for the early warning of thermal runaway and the installation of gas detectors in electric vehicles.

- **Keywords:** Electric vehicles; Thermal runaway; Gas diffusion; Safety warning; Gas detector

Lu-Qing Wang, Dai-Guo Chen, Hong-Hao Ma. *Propagating characteristics of spherical flames in H₂-N₂O mixtures*. Pages 575-584.

The laminar burning velocity and cellular instabilities of premixed flame in H₂-N₂O mixtures were studied experimentally at various equivalence ratios (ϕ) and initial pressures (p_0). High-speed schlieren was used to record the morphology of the spherical flame. Based on the spherical flame method, the laminar burning velocity and Markstein length were derived. In addition, the Lewis number, flame thickness, thermal expansion and Zel'dovich number were evaluated numerically. The results show that both the laminar burning velocity and Markstein length increase with the equivalence ratio. The Lewis number (less than unity) increases with the equivalence ratio while the flame thickness exhibits an inverse evolution. Hence, the most unstable flames were found to be at $\phi=0.4-0.6$ due to the combined effects of the thermal-diffusion and hydrodynamic instabilities. At lower initial pressure, the flame front is smooth in spite of the diffusion-thermal instability. With the increase of initial pressure, both the diffusion-thermal instability and hydrodynamic instability dominate the cellular structure of the flame front. The flames undergo self-acceleration at $\phi=0.4-0.6$ and $p_0=40$ kPa, with the acceleration exponents close to 1.5 (the value of self-turbulization). Due to the local oscillation of velocity, the flame propagation speed decreases after the self-similar regime.

- **Keywords:** Nitrous oxide; Hydrogen; Flame instability; Laminar flame speed; Self-acceleration

Xi Chen, Wenbo Li, Bhupendra Singh Chauhan, Saleh Mahmoud, Wael Al-Kouz, Abir Mouldi, Hassen Loukil, Yong Chen, Salema K. Hadrawi. *Waste heat from a flame-assisted fuel cell for power generation using organic Rankine cycle: Thermoeconomic investigation with CO₂ emission considerations*. Pages 585-598.

The increasing concerns about pollutant emissions from the electricity generation sector have urged the deployment of novel and efficient technologies. In this regard, fuel cells are predicted to be essential in upcoming clean electricity generation systems. In particular, Flame-assisted Fuel Cells (FFCs) are among the new technologies and are envisaged to operate with various fuels; however, their relatively low electrical efficiency is a major drawback. The present research aims at the efficiency improvement of a methane-fueled FFC by recovering its waste heat for additional electricity generation using an Organic Rankine Cycle (ORC). To do so, a combined FFC-ORC framework is developed, and its thermodynamic performance as well as economic and environmental emission characteristics, are modeled. By implementation of parametric analysis, impacts on the performance of design/operating variables were examined. A tri-criteria optimization is also accomplished based on exergy efficiency, electricity cost, and CO₂ emission for the combined FFC-ORC and the standalone FFC. The results indicate better performance of the developed FFC-ORC over the standalone FFC in terms of efficiency and CO₂ emissions, respectively by 8.5-percentage points and 35.2%, under optimized cooperating conditions. However, the electricity cost shows an increment of 9.68% due to the additional expenditures associated with the ORC.

- **Keywords:** Flame fuel cell; ORC; Waste heat recovery; Thermoeconomic; CO₂ emission

Shijun Zhou, Zhenming Zhang, Matthew R. Hipsey, Jiakai Liu, Mingxiang Zhang. *Differences in mass concentration and elemental composition of leaf surface particulate matter: Plant species and particle size ranges.* Pages 599-610.

Leaf surface particulate matter (PM) is an optimal material for the environmental monitoring of urban green spaces. Currently, most studies have looked at leaf surface PM, using only its mass concentration to investigate the dust retention capacity and mechanisms of different plant leaves. The elemental composition of leaf surface PM has been neglected as a reflection of the environment and its sources. Therefore, in this study, ten common plant species were selected from the Olympic Forest Park, an urban green space in Beijing, and the characteristics of leaf surface PM were analysed in depth in terms of mass concentration and elemental composition. The leaf surface PM mass concentration was first obtained by vacuum filtration (VF) method, and then the leaf surface PM attached to the filter membrane obtained from the previous step was used as experimental material to study its elemental composition using cold field emission scanning electron microscopy combined with energy dispersive X-ray spectroscopy (FESEM-EDS). The results show that (1) In terms of mass concentration, *Hemerocallis fulva*, *Poa pratensis*, *Acorus calamus*, *Typha orientalis*, and *Phragmites communis* had better dust retention capacity; (2) The five most important elements deposited on the leaf surface of plants in Beijing were C, O, Mg, Al, and Si, with a total of 26 elements detected; (3) The particulate matter retained on the leaf surface of plants in Beijing was classified as Geogenic particles (57.70%) > Anthropogenic particles (22.30%) > Biogenic particles (20.00%). The results at this stage are expected to promote the in-depth understanding of plant leaf remediation of PM.

- **Keywords:** Leaf surface; Particulate matter; Vacuum filtration; Scanning electron microscopy; Elemental composition; Urban green spaces

Shaomin Liu, Yutao Huang, Juanjuan Peng, Jinglin Zhu. *Efficient degradation of phosphonate via trace Cu(II) mediated activation of peroxymonosulfate.* Pages 611-618.

The phosphonates in wastewater have attracted much attention due to their potential risks to the aquatic environment, which is oxidized to orthophosphate (PO_4^{3-}) is a vital step to achieve their removal. Advanced oxidation processes based on free radicals is usually crucial methods to remove phosphonates, which could be easily disturbed by water matrix. Herein, using 1-hydroxyethane-1,1-diphosphonic acid (HEDP) as a model pollutant, a nonradical system was constructed via Cu(II)/PMS process. 82 % HEDP is degraded by trace Cu(II) ($5 \mu\text{M}$) mediated peroxymonosulfate (PMS) activation process within 60 min at $\text{pH} = 7.0$, which is much higher than that in Cu(II)/peroxydisulfate (PDS) and Cu(II)/ H_2O_2 systems under identical conditions. The results of multiple experiments reveal that Cu(III) inducing intramolecular electron transfer as the dominant reactive species makes responsible for the oxidation of HEDP in the Cu(II)/PMS process, whereas the role of hydroxyl radicals ($\text{HO}\cdot$) and $^1\text{O}_2$ is negligible. In addition, the presence of HCO_3^- , benzoic acid (BA) and phenol shows a negative effect on the oxidation of HEDP in the Cu(II)/PMS process. However, in the actual wastewater, the removal efficiency of HEDP in the Cu(II)/PMS process is much higher than that in other free radical processes (i.e., UV/ H_2O_2 , UV/PDS). This study provides a new idea for the removal of phosphonates from actual wastewater.

- **Keywords:** Phosphonate; Peroxymonosulfate; Cu(II); Selective Oxidation; Intramolecular electron transfer

Chunlong Zhao, Youcai Zhao, Kunsen Lin, Zhengyu Wang, Tao Zhou. *Comprehensive assessment of thermal characteristics, kinetics and environmental impacts of municipal solid waste incineration fly ash during thermal treatment.* Pages 619-631.

The volatilization of heavy metals and the release of harmful gases during the thermal treatment of municipal solid waste incineration (MSWI) fly ash (FA) can cause secondary pollution. Understanding the thermal characteristics, heavy metal behaviors and environmental emissions in FA roasting is significant for pollution control and heavy metal elimination. In this work, the thermodynamics, kinetics, environmental impacts, carbon emission, phase transition, leaching toxicity, transition behavior of chlorine and heavy metals in FA thermal treatment were investigated comprehensively for the first time through TG-FTIR, XRD, ICP-OES and IC. The apparent activation energy and thermodynamic parameters were obtained according to the kinetic modeling method. The average apparent activation energy values of the first, second, third, and fourth stages were 60.21, 114.91, 190.23, and 226.67 kJ/mol, respectively, and the reaction control models were chemical reaction model (No.3), assumed random nucleation and subsequent growth model (No.21), assumed random nucleation and subsequent growth model (No.14), and nucleation model (No.10). The environmental impacts illustrate that large amounts of gaseous products, including CO₂, H₂O, NO and SO₂, are released during the thermal treatment of FA, and the emission of CO₂ sharply increases as the temperature exceeds 550 °C. When treating 1 kg of FA at 1000 °C, the release of CO₂ in stages I, II, III and IV is 0.18, 7.06, 116.34 and 177.21 g, respectively, and the total carbon emission is approximately 300 g. The leaching toxicity of heavy metals in FA is higher below 800 °C, and it is mainly caused by Pb. In addition, the volatilization rate of heavy metals and chlorine increased significantly as the calcination temperature exceeded 800 °C, among which, the volatilization rates of Pb, Cu, and Cl can reach 99.87%, 90.25% and 73.85%, respectively. At high temperatures, heavy metals in FA exist primarily in oxidizable and residual states. The obtained findings can provide theoretical guidance for pollution control and process optimization of FA thermal treatment.

- **Keywords:** Municipal solid waste incineration fly ash; Thermodynamics; Kinetics; Carbon emission; Heavy metals; Mineral phase transition

Jianpeng Wang, Xiaoyang Luan, Jiali Huo, Mingju Jing, Mitchell Huffman, Qingsheng Wang, Bin Zhang. *Numerical study on the effect of complex structural barrier walls on high-pressure hydrogen horizontal jet flames.* Pages 632-643.

Hydrogen has the potential to produce energy with no emissions, and therefore offers a strategic opportunity for rapid development of renewable energy storage. However, jet flames caused by the leakage of high-pressure hydrogen may cause casualties and damage equipment, so the safety issues associated with hydrogen incidents are a key issue restricting its development. Barrier walls can be an important mitigative action to reduce the hazard of hydrogen jet flames. Previous studies have evaluated the protective effect of different vertical or inclined arrangements of a single barrier wall in the vertical direction. However, in the vertical direction, a single barrier wall is not sufficient to reduce the hazards associated with high-pressure hydrogen jet flames. In this paper, a two-dimensional CFD model of high-pressure hydrogen jet flames are established. A simplified form of the hydrogen real gas equation of state is used to describe the complex behavior of high-pressure hydrogen. This CFD study employs the standard k-ε turbulence model, the eddy dissipation concept (EDC) model, and the discrete ordinate (DO) radiation model. The results display good agreement with the experimentally obtained flame shape and thermal radiation values, which confirms the applicability of the model. Based on this model, the characteristics of high-pressure jet flames are systematically

studied under different forms of barrier walls and different pressures of hydrogen storage. Compared with the vertical barrier wall, barrier walls with complex structures can block the flames in front of the wall more effectively. This is proven through a remarkable decline in the vertical flame length and a reduction in the high temperature area. Comparing the five barrier wall patterns for their combined flame shape and flame temperature, it is more preferred to choose 60° Plate. The results of this study will help to better analyze the consequences of hydrogen jet flames and provide guidance for better design of barrier walls for mitigation.

- **Keywords:** Complex structural barrier walls; Hydrogen jet flames; Fluent; Flame temperature; Hydrogen safety

Feihao Zhu, Zegong Liu, An-Chi Huang. *Study on the coupling mechanism of shaped blasting and empty hole to crack coal body.* Pages 644-653.

In this study, the mechanism of cracking under the coupling effect between the use of shaped blasting and deployment of empty holes was explored through theoretical analyses, numerical simulations, and experiments to determine the effects of empty holes on the traveling characteristics of blast-induced stress waves, the propagation patterns of detonation cracks, and the evolution characteristics of blast-induced damage. The results indicated that shaped blasting concentrated energy in a fixed direction to enhance the efficiency of explosive energy use, and the resultant shaped jet created a directional, cut-like crack in the coal layer of specimens. The additional free face provided by empty holes increased the tensile stress, the level of damage in areas located far away from the blast hole, and the propagation capacity of the crack. The levels of specimen damage in shaped blasting that were determined using the resistivity and ultrasonic wave velocity were 1.2 and 1.7 times higher, respectively than those in ordinary blasting. The tensile strain at the empty holes was 2.73 times higher and the static loading phase was 0.9 μ s longer in shaped blasting than in blasting sites without empty holes. The coupling effect between shaped blasting and empty holes substantially improved the effectiveness of the blasting operation in creating directional cracks. This study provides a theoretical and experimental basis for directional blasting techniques; reveals an effective approach that enhances the efficiency of blasting, improves the effectiveness of blast holes, and limits blasting disturbance; and offers socially valuable insights into safe and efficient production practices.

- **Keywords:** Shaped blasting; Empty hole; Blast-induced stress wave; Crack propagation; Safe and efficient production

Xianlong Wang, Qing Zhao, Yuyang Jiao, Kexin Yin, Jifu Zhang, Yinglong Wang, Peizhe Cui, Zhaoyou Zhu. *Process design and comprehensive 3E analysis of low carbon diol production with and without heat integration.* Pages 654-664.

As an important chemical intermediate, the synthesis process of 1,4-butanediol is still energy-intensive and seriously polluting the environment. It is necessary to study its high efficiency and energy saving. The two step synthesis process of 1,4-butanediol: (1) ethynylation of formaldehyde reaction and separation, (2) hydrogenation of 1,4-butynediol reaction and separation are simulated. A sequential iterative optimization method is used to optimize the whole process of 1,4-butanediol production to obtain the best parameters which achieve the minimum annual total cost. In order to further explore the energy-saving process, the heat integration technology is introduced on the basis of the common process, and the annual total cost of the process is reduced by 28.30%. In addition, the exergy efficiency and environmental impact of common process and heat integration process are compared. The results showed that the exergy efficiency of the heat integration process is increased by 6.67% and the CO₂, SO₂ and NO_x emission is reduced by 32.48%, 32.48% and 62.01% compared with the common

process. Through the comprehensive analysis of the economy, exergy and environment of synthesis processes, it has important reference significance for the synthesis of 1,4-butanediol in industry.

- **Keywords:** 1,4-butanediol; Economic; Exergy; Environment; Heat integration process

Anjani R.K. Gollakota, Munagapati Venkata Subbaiah, Chi-Min Shu, Prakash K. Sarangi, Jet-Chau Wen. *Polymer functionalized Hazel Sterculia hydrogel beads for adsorption of anionic azo dye RR120 from industrial streams. Pages 665-676.*

Biomass (Hazel Sterculia seed-HS) was functionalized with chitosan and sodium alginate polymers to synthesize novel sorbent materials for the extraction of anionic reactive red 120 dye molecules from aqueous streams. Sodium alginate functionalized biomass (HSSA) and chitosan functionalized biomass (HSCS) were generated using a 1:1 ratio throughout the functionalization process. Characterization techniques (XRD, FTIR, SEM, and BET) showed that the functionalization process effectively modified the morphological properties of the raw biomass, including an increase in surface area from 1.03 m²/g to 7.81 m²/g (HSCS) and an increase to 5.58 m²/g (HSSA). Similarly, batch adsorption studies were conducted with varying starting dye concentrations (10–1000 mg/L), adsorbent dosages (0.05–0.15 g), contact times (0–360 min), agitation speeds (100–500 rpm), and pH (1–10). The Langmuir and Freundlich isotherm models were used to learn more about the adsorption process. Maximum adsorption capacities of 79.35 mg/g (HSCS) and 60.27 mg/g (HSSA) were observed for Langmuir monolayer adsorption, respectively. In addition, kinetic modeling studies showed that pseudo-second order kinetics, with a regression coefficient of R² > 0.99, was a good fit for RR120 adsorption onto HSCS, HSSA. The thermodynamic properties showed that the adsorption of RR120 onto the selected adsorbents was an endothermic, spontaneous process. Finally, regeneration studies verified that HSCS and HSSA sorbents could be recycled for three, and two cycles respectively.

- **Keywords:** Hazel sterculia; Chitosan; Sodium alginate; Reactive red 120; Adsorption

Ahmed H. Sadek, Ahmed Abdel-Karim, Sajjad Mohsenpour, Sameh H. Ismail, Ahmed M. Bayoumy, Medhat Ibrahim, Gehad G. Mohamed. *Polysulfone-based mixed matrix membranes loaded with a multifunctional hierarchical porous Ag-Cu dendrites@SiO₂ core-shell nanostructure for wastewater treatment. Pages 677-691.*

Eliminating pollutants from wastewater is a crucial approach to securing the global water supply. It is well known that membrane purification technologies are remarkably attractive due to their high efficacy and low energy consumption. The neat polysulfone (PSF) polymer membranes, though, are prone to be fouled by organic pollutants, causing pore blockage and waned separation performance. We herein report and describe the rational design of a hierarchical porous Ag-Cu dendrites@SiO₂ core-shell nanostructure/PSF mixed matrix membranes (MMMs) by coupling heterogeneous dendritic Ag-Cu@SiO₂ core-shell nanostructure with PSF polymer matrix using facile phase inversion method for efficient separation of the protein (Bovine Serum Albumin; BSA) and Rose Bengal (RB) dye removal. Besides, for the first time, a theoretical mapping of molecular electrostatic potential (MESP) maps for chemical structure has been used for studying the interaction between the compounds (membrane moieties and pollutants). Practically, the SiO₂ nanoparticles provide excellent hydrophilicity causing a sequential efficient, antifouling protein and dye separation with an outstanding rejection rate of over 96 % for both BSA and RB. In addition, the porous hierarchical scaffold

formed from the hydrophilic Ag-Cu nanosheets embedded with SiO₂ nanoparticles greatly assists the rapid permeation of water with a high flux rate of up to 50 L m⁻² h⁻¹ bar⁻¹ for pure water. Furthermore, the hydrophilic nature of Ag and Cu nanoparticles also renders this membrane with a high removal capability for dye blocking enabling it to remove soluble pollutants in molecular dimensions as well. This design strategy not only provides an outstanding membrane for water purification but also sheds light on the design of multi-purpose functional membranes for a variety of energy and environment-related applications.

- **Keywords:** Hierarchical pores; Mixed matrix membranes; Wastewater; Protein separation; Dye removal; MESP

Jie Zhang, Demeng Qian, Han Zhang, Jianye Wang, Xuanyao Wang, Shanghao Liu. *Research on the thermal hazard characteristics of 1-propyl-3-methylimidazolium nitrate and risk assessment. Pages 692-699.*

The application of ionic liquids is prevalent in various industries, including pharmaceutical, chemical, and aerospace, especially in environments with high temperatures. Thus, the importance of researching the characteristics and mechanism of the pyrolysis hazard of ionic liquids cannot be overemphasized. This research presents a systematic study of a new versatile ionic liquid, 1-propyl-3-methylimidazolium nitrate ([Pmim][NO₃]). The flash-ignition temperature, thermal decomposition and thermal runaway characteristics of [Pmim][NO₃] were analyzed using various techniques, including thermogravimetric analyzer, differential scanning calorimetry, flash-ignition temperature tester, and accelerating rate calorimeter, for determining its major hazard characteristics. The main thermodynamic and safety parameters, as well as the reaction pattern of the pyrolysis process, were obtained. Additionally, an assessment was conducted to determine the potential occurrence and seriousness of a runaway reaction of [Pmim][NO₃] decompose. The present study is of significant importance in improving the intrinsic safety level of ionic liquids in the processes of synthesis, utilization, storage, and transportation.

- **Keywords:** Ionic liquids; Thermal decomposition; Thermal runaway; Thermodynamic and safety parameters; Reaction pattern

Ramon Swell Gomes Rodrigues Casado, Marcelo Hazin Alencar, Adiel Teixeira de Almeida. *Portfolio-based decision model for enhancing the mitigation of multidimensional risks in hydrogen pipeline sections. Pages 700-714.*

In exploring alternative and more sustainable sources, hydrogen has played a dominant role as an energy vector and is suitable for reducing carbon emissions. However, given the properties of hydrogen and existing transportation challenges for this substance, studies that involve assessing risk when transporting hydrogen still need attention. Therefore, this paper presents a multi-criteria decision model to support organizations responsible for transporting hydrogen in a pipeline in risk management under a multidimensional perspective. In particular, we developed a search algorithm to select sections within the set that makes up the pipeline network (a portfolio-based approach), with a view to identifying the most critical areas in terms of risks and to optimizing the allocation of resources for mitigation while respecting current requirements. In addition, these risks are evaluated under three dimensions of loss: environmental, financial, and human. Hence, a numerical application is presented to illustrate the benefits of the model proposed. The results demonstrate that the model can help managers make more informed and strategic decisions about where to direct their risk management efforts to maximize pipeline safety and minimize incident risks.

- **Keywords:** Hydrogen pipeline; Multidimensional risk; Risk management; Portfolio-based approach; Multi-criteria decision model

Jiapeng Li, Jinghong Wang, Jun Xie, Juncheng Jiang. *Risk assessment of lithium-ion battery road transportation using the data-driven Bayesian network considering battery self-heating. Pages 715-731.*

As a key component in electric vehicles or electronic devices, highly flammable lithium-ion batteries have been a growing concern for transportation safety, as evidenced by a number of lithium-ion battery fires in vehicle containers. Therefore, it is important to assess the key risk factors for fire accidents during the transportation of lithium-ion batteries. This study proposes a dynamic Bayesian assessment model for the transport risk assessment of lithium-ion batteries considering battery self-heating. A simulation model is constructed to explore the self-heating law of lithium-ion batteries and quantify their self-heating risk during transportation process. Based on Bayesian networks, a lithium-ion battery transportation risk assessment model is constructed by combining historical accident data and expert knowledge. The prediction results show that transportation accidents become more severe as transportation time increases. After four hours of transportation, the risk value was 12.28 % higher than that at the beginning. The battery self-heating and the improper handling are the most likely risk factor for fatal accidents, with a probability of 92.2 % and 72.4 % respectively, and these two risk factors have a great influence on accident severity. The mutual information of the ambient temperature is nearly four times that of the critical ambient temperature, indicating the ambient temperature is the key factor influencing the battery self-heating. This work aims to provide a theoretical basis for improving battery safety and reducing hazards during transportation.

- **Keywords:** Risk assessment; Bayesian networks; Lithium-ion battery; Self-heating

Chih-Ping Lin, Yin Jeh Ngui, Yi-Pei Chan, Albert T. Yeung. *Feasibility of a TDR-based technique for fluid hydrocarbon leak detection. Pages 732-743.*

Undetected leakage of fluid hydrocarbons from pipelines or underground storage tanks into the subsurface environment are environmental and public health hazards. It is evident that there is a need for efficient, effective and accurate technology to detect these leaks rapidly and non-destructively, so as to make the process safe, to make quantitative risk assessment, and to provide effective preventive measures. There are unsurmountable limitations in many existing leak detection techniques. Moreover, early detection of leakage would allow rapid remediation at source to significantly reduce the remediation costs, and more importantly the environmental impact. The results of an experimental investigation for the technical feasibility and practicality of a technique for detection and location of fluid hydrocarbon leaks in underground pipelines and storage tanks based on the principles of time-domain reflectometry (TDR) are presented in this paper. The measurement sensitivity of the technique was evaluated for 3 different types of cables, 2 cable configurations (parallel-wires or coaxial), 2 leaking fluids (tap water or petrol), a single leak or double leaks, and 2 backfill materials (fine sand or gravel) by a series of field-scale model tests. The testing parameters were varied systematically. The experimental results indicate that TDR is a technically feasible technique for the detection of fluid hydrocarbon leaks from pipelines and underground storage tanks when the setup configuration is appropriate.

- **Keywords:** Fluid hydrocarbon leak; Time-domain reflectometry (TDR); Leak detection; Pipeline; Underground storage tanks; Dielectric constant; Dielectric permittivity

K. Muthukumar, G. Kasiraman. *Downcycling of one-time used plastic waste to DICI engine combustion energy through pyrolysis with less NOx emission. Pages 744-752.*

Plastic waste elimination is more important for environmental pollution. Alternate fuel is essential for future IC engine applications because of fossil fuel availability. This study focuses on both challenges by creating combustion energy for direct injection CI engines from the wastes with lesser NO_x emissions. Plastic wastes of low-density polyethylene (LDPE) have the most negligible recycling value based on their collection point of view from municipal wastes. Conversion of this LDPE plastic waste into alternate fuel for CI engines by pyrolysis will provide value for that waste. The combustion, emission, and performance of neat pyrolyzed oil of LDPE plastic wastes (POLPW) were studied with exhaust gas recirculation (EGR; 0%, 10%, and 20%) in a 1500 rpm 5.2 kW engine on different loads. 20% of EGR used POLPW fuel produced 31.63% of brake thermal efficiency and 62.28% reduction in NO_x (596 ppm) than diesel at maximum load. Pyrolyzed oil of low-density polyethylene plastic wastes can be utilized as a 100% substitute fuel in CI engines with an EGR of 20%. This will provide alternate fuel and low-value plastic waste downcycling, initiating environmental pollution reduction.

- **Keywords:** Waste to energy; plastic waste; low-density polyethylene; plastic pyrolysis oil; alternative fuel; emission on CI engine

Haotian Zheng, Bingyou Jiang, Yuannan Zheng, Yang Zhao, Haoyu Wang. *Experimental study on forced ventilation and dust -control in a heading face based on response surface method. Pages 753-763.*

Aiming at the problems of unreasonable air flow distribution and serious dust pollution in roadway under forced ventilation of coal mine in a heading face, this study conducted experimental research based on response surface method, and effectively reduced dust concentration by changing air flow distribution in roadway. Firstly, a single factor experiment was conducted to explore the impacts of air outlet wind speed (V_a), distance from air outlet to heading face (LS), and driving height (H_d) on the dust concentration at the position of the driver (Y_1) and the height of the pedestrian breathing belt (Y_2). Subsequently, a comprehensive air flow control response surface test was designed based on the Box-Behnken principle to optimize the dust field, with Y_1 and Y_2 as the response index. Finally, the sequence of the impact of each variables on the dust concentration and the optimal air flow scheme were determined through the response surface method. The test results showed that the order of significance of Y_1 was $H_d > V_a > LS$, and the order of significance of Y_2 was $LS > V_a > H_d$. The maximum error between the test value and the predicted value in the optimization model is only 4.01%, the dust concentration at the driver's position and the pedestrian's breathing belt height decreased by 57.7% and 53.8%, respectively, and the dust-control effect was obvious.

- **Keywords:** Heading face; Forced ventilation; Air flow control; Dust field optimization; Response surface method

Muhammet Yilanli, Mohammad Rauf Sheikhi, Onder Altuntas, Emin Açıkkalp. *Assessing the global warming potential of aircraft gas turbine materials: Impacts and implications. Pages 764-773.*

The aviation industry generates a wide range of climate pollutants, which often leads to an underestimation of its impact on global warming. Constructing aircraft components using environmentally friendly materials could significantly reduce the environmental burden associated with aviation growth. The objective of this study is to evaluate the Global Warming Potential (GWP) of commonly used alloys in gas turbine engines of aircraft. Material information on aircraft engine components was extracted, and GWP

data for each metal was obtained using SimaPro software, and the GWP of components was determined. The study revealed that RENE 15 and GTD111 turbine alloys had the highest GWP impact, ranging from 13.53 to 14.05 kg CO₂e/kg, while AISI 403 and GTD-450 used in the compressor, M152 used in the turbine, and Cr-Mo-V alloys used in both the turbine and shafts had the lowest GWP effect, ranging from 1.61 to 1.90 kg CO₂e/kg. Moreover, the study evaluated the environmental impact associated with the manufacturing of aircraft engine components. The findings indicated that Ti-based materials had the highest GWP rate, with a value of 3.29 kg CO₂e/kg, which was almost the sum of all other metals. In particular, Ti-based materials used in fan components were identified as the largest source of environmental impact during aircraft engine production, with a value of 2.02 kg CO₂e/kg. These results underscore the crucial role of material selection in mitigating environmental impacts during aviation engine component production. The study highlights the need for more effective and efficient approaches to material selection from an environmental standpoint in the aviation industry, especially in the context of reducing global warming potential. The results of this research could inform decision-making related to material selection for aircraft engine components, and help the aviation industry to reduce its overall environmental impact and mitigate the effects of global warming.

- **Keywords:** Global warming potential; Aircraft engine materials; Gas turbine engine components

Huiyang Bi, Chunhui Deng, Lihao Chen, Xuesong Zhao, Zhongjian Li, Yang Hou, Lecheng Lei, Bin Yang. *Numerical simulation study on the formation and control of HCl during the gasification of industrial organic hazardous waste. Pages 774-782.*

The utilization of industrial organic waste instead of coal by high temperature gasification to produce syngas is a promising way to reduce carbon emissions. The distinct property of industrial hazardous waste is characterized as high content of chlorine and volatile organics, which is significantly different from coal-water slurry. Herein, novel numerical models were established to simulate the formation and control of HCl in the Texaco gasifier, where the chlorine-containing substances were simplified as dichloromethane to describe the mass transfer during the gasification. The models presented a good accuracy with the minimum error of 0.55% in syngas components prediction. The simulation demonstrated that HCl was generated near the nozzle, and the increasing of CaO amount and the decreasing of its particle size had positive effect on dechlorination. However, excessively reducing the size of CaO below 0.1 mm decreased its promoting effect, and high temperature in flame zone inhibited the dechlorination reaction. Therefore, the models developed in this work provided the feasibility of the general numerical simulation method to optimize the operating conditions in order to reduce the corrosion of chlorine to equipment and improve the stability of operation during the gasification process of organic hazardous waste.

- **Keywords:** Waste utilization; Gasification furnace; Numerical simulation; Organic hazardous wastes; Dechlorination effect

Jianzi Liu, Mingyue Yang, Bhupendra Singh Chauhan, Mostafa Abdrabboh, Mohamed Fayed, Hamdi Ayed, Abir Mouldi, Yong Chen, Xi Chen. *A comparison of two schemes for pure hydrogen injection into a syngas-fueled SOFC: Thermo-economic and environmental-based investigations. Pages 783-795.*

The solid oxide fuel cells (SOFCs) driven by bio-syngas from biomass gasification are among the novel technologies for efficient and clean electricity generation. One challenge facing these systems is the shortage of biomass resources in some seasons and

locations. One solution to mitigate this challenge is hybridizing these systems with other forms of renewable energies for decreasing the biomass consumption. The present work proposes integration of biomass driven SOFC with wind energy, in which the extra hydrogen is produced using the wind turbines and is used as a co-feed fuel for the SOFC. The hydrogen is supposed to be produced using an alkaline electrolyzer driven by electricity from the wind turbines. Two structural configurations are developed regarding how the extra hydrogen is injected into the basic biomass fueled SOFC. In one system the produced hydrogen is mixed with syngas fuel before the anode entry, while in the other system the hydrogen is burnt in afterburner of the SOFC for more power generation in the integrated gas turbine. Practical feasibility of these hybrid configurations are appraised based on thermodynamics laws, after which their economics and environmental features are investigated. Finally, tri-objective optimization is employed for finding the best operating conditions of the two configurations. According to the obtained results, injecting the extra hydrogen into the anode of the SOFC yields 8.3 % more electricity compared to the other configuration. As a result of more electricity generation, it yields 5.4 % less environmental emissions and 7.9 % less unit electricity cost.

- **Keywords:** Biosyngas; SOFC; Wind energy; Hydrogen; Economic

Junlin Huang, Nengwu Zhu, Xiang Li, Yunhao Xi, Weiqing Shen, Pingxiao Wu. *Triggered heavy metals and chlorine simultaneous removal from hazardous waste incineration fly ash.* Pages 796-805.

To date, heavy metals and chlorine removal from hazardous waste incineration fly ash (HWI FA) by thermal treatment was scarcely reported. High content of calcium in HWI FA might affect heavy metals chlorination volatilization. The aim of this study was to realize heavy metals and chlorine simultaneous removal from HWI FA triggered by fluidized-bed municipal solid waste incineration fly ash (FBMSWI FA) during sintering. Results showed that the dilemma of low heavy metals removal efficiency was due to the dense structure and the difficulty of transformation of the stable phases including Cu_2S , CuSiO_3 , and Zn_2SiO_4 . By co-sintering with FBMSWI FA at the ratio of 1:1, the removal efficiency of Cu, Zn, Pb, Cd, and Cl reached as high as 84.4%, 92.0%, 99.9%, 99.5%, and 99.7%, respectively. Compared with the control, chlorination volatilization efficiency of Cu and Zn was significantly increased by 210.5% and 89.2%. The favourable promotion could be mainly attributed to Si/Al matrix in FBMSWI FA triggered the following reaction: i) Ca-bearing compounds in HWI FA were activated to destroy the dense structure, which facilitated the transformation of Cu_2S to CuO ; and ii) the conversion of NaCl and KCl to gaseous chlorine was promoted, which the formation of metal chlorides was accelerated.

- **Keywords:** Hazardous waste incineration fly ash; Fluidized-bed municipal solid waste incineration fly ash; Thermal disposal; Heavy metals; Chlorination volatilization

Yunhe Qu, Yujia Zhai, Chi Ma, Wansheng Shi, Mingxing Zhao, Zhenxing Huang, Wenquan Ruan. *Rapid start-up of anaerobic digestion reactor with rice-straw ash addition for treating high salinity organic wastewater.* Pages 806-813.

Anaerobic digestion is an economic method to treat high-salinity organic wastewater (HSOW). However, due to the inhibitory effect of high salinity, the start-up of the anaerobic digestion reactor is slow and easy to fail. In this study, as a potassium source, rice-straw ash (RSA) was used to enhance the HSOW treatment performance and shorten the start-up time of anaerobic digestion reactor under 3.0% NaCl content and high loading rate. The results showed that RSA could provide adequate potassium ion (K^+) for alleviating the inhibitory effect of high salinity on anaerobic microorganisms. The

rapid start-up of the anaerobic digestion reactor was realized, and the TOC removal rate reached 81.65%. In the reactor with RSA addition, the activities of dehydrogenase, acetic kinase and coenzyme F420 were 25.67%–89.81%, 19.03%–50.93% and 35.83%–944% higher than that of the control reactor, respectively. The addition of RSA promoted the accumulation of acetoclastic methanogen *Methanotrix*, and changed the methanogenic pathway from hydrogenotrophic methanogenesis in the beginning stage of anaerobic digestion to acetoclastic methanogenesis under high salinity condition. After stopping the addition of RSA, the performance of the anaerobic digestion reactor remained stable, indicating that RSA was only needed at the start-up stage. This study could provide a feasible method for rapid start-up of anaerobic digestion reactor treating HSW in practice.

- **Keywords:** High salinity organic wastewater; Anaerobic digestion; Rice-straw ash; Biogas production; Rapid start-up of reactor

Liangli Zhang, YiFei Qiu, Yun Chen, Anh Tuan Hoang. *Multi-objective particle swarm optimization applied to a solar-geothermal system for electricity and hydrogen production; Utilization of zeotropic mixtures for performance improvement. Pages 814-833.*

Renewable energy sources such as solar, wind, and geothermal energy have become increasingly popular due to their environmental benefits and long-term sustainability. This study proposes an innovative integration of a solar system and a geothermal system to optimize the performance of a geothermal power plant. The geothermal system is coupled with a solar system, which utilizes a direct and storage system to increase the efficiency of solar energy utilization and minimize energy loss. To recover waste heat, an electrolyzer is used in a triple-flash geothermal system that operates at high feed geofluid temperatures, producing hydrogen as a byproduct. The organic Rankine cycle with a zeotropic mixture working fluid is employed to generate additional power. After considering eight candidate working fluids, Butene/R123 is selected. The designed system exhibits an impressive 10.83 MW net power, 9.87 kg/h hydrogen, 18.86% energetic efficiency, 29.45% exergetic efficiency, and 4.88 years payback period with a 29.72 M\$ net present value. Additionally, two energy-economic and exergy-economic scenarios are evaluated to determine the optimum state. The energy-economic scenario has a lower payback period, whereas the exergy-economic scenario offers greater profitability over the system's lifetime.

- **Keywords:** Triple-flash cycle; Solar and geothermal integration; Zeotropic mixture; Working fluid selection; Payback period and profitability evaluation

Ya You, Shuang-Ning Li, Jiao Zou, Ya-Nan Xin, Sui Peng, Bo Liu, Xin-Yu Jiang, Jin-Gang Yu. *Ultrasonic-assisted self-assembly of a neodymium vanadate and hydroxylated multi-walled carbon nanotubes composite for electrochemical detection of p-nitrophenol. Pages 834-844.*

In recent years, nanocomposites prepared from rare earth metal vanadate and carbon nanomaterials have attracted great attention, and they have shown great promise for electrochemical sensing applications. Herein, a facile ultrasonic-assisted assembly method was adopted to prepare neodymium vanadate/hydroxylated multi-walled carbon nanotubes (NdV/MWCNTs-OH) composite. The morphology, elemental states, crystal structure and functional groups of the composites were investigated through a series of characterizations. Then, a novel electrochemical sensor, NdV/MWCNTs-OH composite modified glassy carbon electrode (GCE), was designed for the detection of p-nitrophenol (PNP). The synergistic effect generated by the combination of NdV and MWCNTs-OH accelerated the charge transfer kinetics and exposed more active sites, which facilitated more effective detection. Under optimized experimental conditions, the as-prepared

sensor exhibited a wider linear range (1–200 μM) to PNP, and a lower limit of detection (LOD) of 0.41 μM could be obtained (signal-to-noise ratio of 3; $S/N = 3$). Furthermore, the sensor was successfully used for the determination of PNP in real samples (industrial wastewater and river samples), and satisfactory recoveries (96.67%–101.88%) with RSDs less than 5% were observed. Herein, the prepared electrochemical sensor has potential application prospect in the analysis and detection of PNP.

- **Keywords:** Electrochemical sensor; Neodymium vanadate; Hydroxylated multi-walled carbon nanotubes; Assembled composite; P-Nitrophenol

Yan Pei, Wei Wang, Xun Liu, Mengbo Cao, Ming Gao, Yongsheng Li, Hongbing Yang. *Self-propagating combustion synthesized magnetic cobalt carbohydrate-based adsorbents for tetracycline elimination.* Pages 845-853.

Herein, a series of adsorbent magnetic cobalt carbohydrate-based (carbon source: glucose, maltose, and starch) carbon adsorbents (Co-Cs) can be rapidly prepared for the removal of tetracycline (TC) from water using a self-propagating combustion method. The results of batch adsorption experiments show that the composites exhibit excellent adsorption performance (maximum adsorption capacity of 430.54 mg/g) towards TC in a wide pH range of 2–10. As the concentration of humic acid (2–10 mg/L) increased, its adsorption capacity enhanced from 176.51 to 281.63 mg/g by forming bridge bonds. Pseudo-second-order kinetic and Freundlich models are more suitable for describing adsorption data. In addition, the hydrogen bond, complexation, and conjugation effect were the major adsorption mechanisms. The adsorption experiments of high concentration TC water samples were tested with hospital wastewater (adsorption capacity up to 236.31 mg/g), which provided some guidance for further practical application. The proposed synthetic strategy provides an efficient, excellent versatility and energy saving method for the preparation of high-performance magnetic adsorbents.

- **Keywords:** Self-propagating combustion; Co-loaded biochar; Magnetism; Adsorption; Tetracycline

Jiaqi Zhi, Yue Yu, Qingshun Zeng, Changfeng Shi, Shiyu Chen, Yuze Wang. *Multi-scale near-long-range flow measurement and analysis of virtual water in China based on multi-regional input-output model and machine learning.* Pages 854-869.

At present, China is facing a relatively serious water security problem, and virtual water trade is an important means to alleviate the shortage of water resources. It is of great practical significance for China to analysis of the multi-scale near-long-distance flow of virtual water between regions. In this paper, the multi-regional input-output model was used to measure the virtual water near-long-range transfer of 17 departments in eight regions in 2012 and 2017 in China. The measured results are further discussed in the context of K-means and structural decomposition analysis (SDA) methods. The results show that from 2012 to 2017, the overall trend of interregional virtual water flow and import and export volume of various regions and departments in China showed a downward trend, and there were significant differences in inflow, outflow, and distribution. In 17 sectors, the agricultural sector has a much higher virtual water flow than other sectors, particularly in the north-west and central regions. In addition, the food and tobacco industry and construction industries in most regions also have the characteristics of high outflows. This paper argues that China should Fully exploit the effect of industrial structure on the suppression of virtual water rise. At the same time, it is necessary to improve the virtual water trade pattern, especially the virtual water trade pattern of the agricultural sector, and then gradually optimize the distribution pattern of regional water resources in China.

- **Keywords:** Water footprint; Virtual water transfer; Virtual water trade; Multi-regional input-output model; K-means

Feng Zhou, Wenhua Cui, Lei Yang, Jinwei Chen. *Proposal of an environmental-friendly poly-generation model regarding the flue gas processing for the production of electricity, cooling, heating, freshwater, and methanol.* Pages 870-891.

In this paper, a novel poly-generation system with high thermodynamic performance and low carbon dioxide (CO₂) emission is presented and analyzed from the 4E (energy, exergy, economic, and environmental) perspective. The newly designed structure consists a gas turbine cycle, transcritical CO₂ cycles, a Kalina power cycle, a water desalination unit, a methanol production unit, and a chiller. Toward this goal, the flue gas leaving the gas turbine cycle is processed and utilized. Thermodynamic analysis demonstrates that the total energy and exergy efficiencies are attainable at 58.75% and 69.46%, respectively. In addition, the total exergy destruction rate equals 183105 kW in which the gas turbine cycle is the major source of irreversibility with a share of 51%. In addition, exergy analysis indicates that the combustor of the gas turbine cycle has the highest exergy destruction ratio (44.54%) among all equipment. Regarding the environmental aspect, the total CO₂ emission and its emission intensity for the proposed process are 18678.42 kgCO₂/h and 0.75 kgCO₂/kgMeOH, respectively. Its indirect emission is responsible for 48.8% of the total emission as well. Attributable to the thermo-environmental results, the proposed process has a suitable performance compared to similar technologies. The economic analysis demonstrated that its total annual cost equals 60800563 \$ and production costs of methanol, freshwater, heating, cooling, and power are 0.3 \$/kgMeOH, 0.43 \$/kgfreshwater, 0.16 \$/kgLPS, 0.022 \$/kgchilled water, and 0.069 \$/kWh, respectively.

- **Keywords:** 4E analysis; Desalination; Flue gas; Methanol production; Poly-generation; Transcritical carbon dioxide